MATHEMATICS OF COMPUTATION
Volume 91, Number 334, March 2022, Pages 735–760
https://doi.org/10.1090/mcom/3721
Article electronically published on January 25, 2022

STRICTLY CONVEX ENTROPY AND ENTROPY STABLE SCHEMES FOR REACTIVE EULER EQUATIONS

WEIFENG ZHAO

Abstract. This paper presents entropy analysis and entropy stable (ES) finite difference schemes for the reactive Euler equations with chemical reactions. For such equations we point out that the thermodynamic entropy is no longer strictly convex. To address this issue, we propose a strictly convex entropy function by adding an extra term to the thermodynamic entropy. Thanks to the strict convexity of the proposed entropy, the Roe-type dissipation operator in terms of the entropy variables can be formulated. Furthermore, we construct two sets of second-order entropy preserving (EP) numerical fluxes for the reactive Euler equations. Based on the EP fluxes and the Roe-type dissipation operators, high-order EP/ES fluxes are derived. Numerical experiments validate the designed accuracy and good performance of our schemes for smooth and discontinuous initial value problems. The entropy decrease of ES schemes is verified as well.

1. Introduction

This paper is concerned with the reactive Euler equations describing inviscid compressible flow with chemical reactions, which are fundamental for modeling detonations. In one dimension (1D), these equations read as [9, 12]

$$\partial_t \begin{pmatrix} \rho \\ \rho u \\ \rho E \\ \rho Y \end{pmatrix} + \partial_x \begin{pmatrix} \rho u \\ \rho u^2 + p \\ \rho E u + p u \\ \rho u Y \end{pmatrix} = \begin{pmatrix} 0 \\ 0 \\ 0 \\ \omega \end{pmatrix}, \tag{1.1}$$

where ρ is the fluid density, u is the velocity, p is the pressure, E is the total energy and Y is the reactant mass fraction. The source term is assumed to be in an Arrhenius form

$$\omega = -\tilde{K}\rho Y e^{-\tilde{T}/T},$$

where $T = p/\rho$ is the temperature, $\tilde{T} > 0$ is the activation constant temperature and $\tilde{K} > 0$ is a constant rate coefficient. The equation of state is $\rho E = \frac{1}{2}\rho u^2 + \frac{p}{\gamma - 1} + q\rho Y$ with $q > 0$ the heat release of reaction and γ the specific heat ratio.

Generally, for N chemical species there should be N species conservation equations for Y_i, $i = 1, 2, \ldots, N$, with Y_i being the mass fraction of species i. The above reactive Euler equations (1.1) are a simplified form under the assumption that there are only two species present, reacted and unreacted species, and that

Received by the editor June 26, 2021.
2020 *Mathematics Subject Classification.* Primary 65M06; Secondary 76M20.
Key words and phrases. Reactive Euler equations, strictly convex entropy, entropy preserving fluxes, entropy stable schemes.

the unreacted species is converted to reacted species by a one-step irreversible chemical reaction [10, 12]. Though relatively simple in form, (1.1) can give complicated stable and unstable wave patterns, which have been observed in experiments [4, 10]. Due to the practical importance, the reactive Euler equations have been widely investigated both theoretically and numerically in the past decades; see e.g. [4, 7, 9, 10, 13, 20, 21, 33].

Eqs. (1.1) are a system of hyperbolic balance laws and degenerate to the Euler equations when $Y = 0$. For these equations as hyperbolic systems, it is well known that entropy conditions are necessary to determine the correct weak solution across a shock. Then it is natural for corresponding numerical schemes to satisfy a discrete version of the entropy condition in computations. Actually, such schemes for hyperbolic conservation laws have been well developed since the pioneer work of Osher and Tadmor [26, 27, 31, 32]. In particular, Tadmor [31] proposed a framework to construct second-order entropy conservative (EC) fluxes, which are locally consistent with the given entropy conservation. Furthermore, entropy stable (ES) fluxes are obtained by adding dissipation operators to the EC fluxes [31]. Using these fluxes as building blocks, high-order EC/ES schemes are designed in [25] and [17]. Though the framework in [31] is quite general, some additional efforts are needed to obtain explicit expressions of the EC fluxes. This issue is addressed in [22, 28] for the compressible Euler equations by choosing a suitable set of algebraic variables. Following the procedure of [22, 28], EC fluxes are derived for the shallow water equations [15], magnetohydrodynamic systems [6, 34, 35] and relativistic hydrodynamics [11]. Moreover, numerical fluxes that are both EC and kinetic-energy preserving (KEP) are proposed in [5] for the Euler equations. Except for those based on the framework in [31], ES schemes have also been developed via the summation-by-parts property; see e.g. [8, 14, 18, 19].

In this paper, we aim to construct ES finite difference schemes for the reactive Euler equations in both one- and two-dimensions on a Cartesian mesh. First, we point out that the thermodynamic entropy is no longer strictly convex for the reactive Euler equations. To address this issue, we propose a strictly convex entropy function by adding an extra term ρY^2 to the thermodynamic entropy. As a result, a new entropy-entropy flux pair is obtained for the reactive Euler equations. Thanks to the strict convexity of the proposed entropy, the Roe-type dissipation operator in terms of the entropy variables can be formulated [28]. Note that such dissipation operators are not available based on the thermodynamic entropy, as it is not strictly convex. Additionally, for the reactive Euler equations as hyperbolic balance laws, the strict convexity of entropy function is crucial for the global existence of solution [36]. The present strictly convex entropy may be helpful for the theoretical analysis of the reactive Euler equations.

Furthermore, we construct two sets of second-order entropy preserving (EP) fluxes by extending those in [5, 28] for the Euler equations within the framework of [31]. Here we use EP instead of EC due to the source term in the entropy equation. In particular, the EP fluxes extended from [5] are also KEP. With the EP fluxes and the above Roe-type dissipation operators, high-order EP/ES fluxes are derived following [17, 25], where the sign-preserving ENO [16] and WENO [3] reconstructions are employed for high-order dissipation operators. Numerical experiments in 1D and 2D not only validate the designed accuracy of our schemes but also demonstrate

their good performance for problems with discontinuities. The entropy decrease of ES schemes is verified as well.

The rest of the paper is organized as follows. In Section 2, we present a strictly convex entropy for the reactive Euler equations. In Section 3, we derive ES schemes in 1D and extensions to 2D are given in Section 4. Section 5 provides some numerical experiments to validate our schemes. Finally, some conclusions and remarks are given in Section 6.

2. Strictly convex entropy for reactive Euler equations

2.1. **1D case.** The 1D reactive Euler equations (1.1) can be written as

$$\partial_t U + \partial_x F(U) = Q(U), \tag{2.1}$$

where

$$U = \begin{pmatrix} \rho \\ \rho u \\ \rho E \\ \rho Y \end{pmatrix}, F(U) = \begin{pmatrix} \rho u \\ \rho u^2 + p \\ \rho E u + p u \\ \rho u Y \end{pmatrix}, Q(U) = \begin{pmatrix} 0 \\ 0 \\ 0 \\ \omega \end{pmatrix}.$$

Let $s = \ln(p) - \gamma \ln(\rho)$ be the thermodynamic entropy and define

$$\hat{\eta} = \frac{-\rho s}{\gamma - 1}, \quad \hat{\phi} = \frac{-\rho u s}{\gamma - 1}, \tag{2.2}$$

which are the classical entropy and entropy flux for the Euler equations, respectively. It is direct to verify for the reactive Euler equations (2.1) that

$$\partial_t \hat{\eta} + \partial_x \hat{\phi} = \frac{\rho}{p} q \omega \leq 0, \tag{2.3}$$

which implies that $(\hat{\eta}, \hat{\phi})$ may be an entropy-entropy flux pair for (2.1). However, for (2.1) $\hat{\eta}$ is no longer strictly convex. To see this, we compute

$$\hat{\eta}_U := \frac{\partial \hat{\eta}}{\partial U} = \begin{pmatrix} \frac{\gamma - s}{\gamma - 1} - \frac{\rho u^2}{2p} \\ \frac{\rho u}{p} \\ -\frac{\rho}{p} \\ q\frac{\rho}{p} \end{pmatrix}.$$

Note that the third and fourth entries of $\hat{\eta}_U$ are proportional. Then the third and fourth rows of the Hessian matrix $\hat{\eta}_{UU}$ are proportional and thus $\hat{\eta}_{UU}$ is singular. This indicates that $\hat{\eta}$ is not strictly convex.

To address the above problem, we propose the following entropy-entropy flux pair

$$\eta = \hat{\eta} + \rho Y^2, \quad \phi = \hat{\phi} + \rho u Y^2 \tag{2.4}$$

by adding ρY^2 and $\rho u Y^2$ to $\hat{\eta}$ and $\hat{\phi}$, respectively. It follows from the first and fourth equations of (2.1) that

$$\partial_t(\rho Y^2) + \partial_x(\rho u Y^2) = 2Y\omega \leq 0.$$

With this and (2.3), we have

$$\partial_t \eta + \partial_x \phi = (q\frac{\rho}{p} + 2Y)\omega \leq 0. \tag{2.5}$$

On the other hand, the corresponding entropy variable of η is

$$V := \eta_U = \begin{pmatrix} \frac{\gamma-s}{\gamma-1} - \frac{\rho u^2}{2p} - Y^2 \\ \frac{\rho u}{p} \\ -\frac{\rho}{p} \\ q\frac{\rho}{p} + 2Y \end{pmatrix} \tag{2.6}$$

and the Hessian matrix is given by

$$\eta_{UU} = \begin{pmatrix} \frac{\gamma}{\gamma-1}\frac{1}{\rho} + (\gamma-1)\frac{\rho u^4}{4p^2} + 2\frac{Y^2}{\rho} & -(\gamma-1)\frac{\rho u^3}{2p^2} & -\frac{1}{p} + (\gamma-1)\frac{\rho u^2}{2p^2} & q\frac{1}{p} - (\gamma-1)q\frac{\rho u^2}{2p^2} - 2\frac{Y}{\rho} \\ -(\gamma-1)\frac{\rho u^3}{2p^2} & \frac{1}{p} + (\gamma-1)\frac{\rho u^2}{p^2} & -(\gamma-1)\frac{\rho u}{p^2} & (\gamma-1)q\frac{\rho u}{p^2} \\ -\frac{1}{p} + (\gamma-1)\frac{\rho u^2}{2p^2} & -(\gamma-1)\frac{\rho u}{p^2} & (\gamma-1)\frac{\rho}{p^2} & -(\gamma-1)q\frac{\rho}{p^2} \\ q\frac{1}{p} - (\gamma-1)q\frac{\rho u^2}{2p^2} - 2\frac{Y}{\rho} & (\gamma-1)q\frac{\rho u}{p^2} & -(\gamma-1)q\frac{\rho}{p^2} & (\gamma-1)q^2\frac{\rho}{p^2} + \frac{2}{\rho} \end{pmatrix}. \tag{2.7}$$

The positive definiteness of the above matrix is proved as follows. Additionally, the entropy potential of the entropy-entropy flux pair (η, ϕ) can be computed as $\psi := V^T F - \phi = \rho u$, which is the same as that for the Euler equations. Here the superscript T stands for the transpose operator.

Theorem 2.1. *The Hessian matrix η_{UU} in* (2.7) *is positive definite. Namely, the entropy function η in* (2.4) *is strictly convex.*

Proof. We prove this by showing that all the leading principal minors of η_{UU} are positive. Note that the leading principle 3×3 submatrix of η_{UU} is actually $\mathsf{A}_3 := \mathsf{A}_{\text{Euler}} + \text{diag}(2\frac{Y^2}{\rho}, 0, 0)$, where $\mathsf{A}_{\text{Euler}}$ is the Hessian matrix of the classical entropy $\hat{\eta}$ for the Euler equations and thereby is positive definite. Then A_3 is positive definite and the first three leading principal minors of η_{UU} are positive. Next we only need to show that the fourth leading principal minor, i.e., the determinant of η_{UU}, is positive. To do this, we compute

$$\begin{aligned} |\eta_{UU}| &= \begin{vmatrix} \frac{\gamma}{\gamma-1}\frac{1}{\rho} + (\gamma-1)\frac{\rho u^4}{4p^2} + 2\frac{Y^2}{\rho} & -(\gamma-1)\frac{\rho u^3}{2p^2} & -\frac{1}{p} + (\gamma-1)\frac{\rho u^2}{2p^2} & q\frac{1}{p} - (\gamma-1)q\frac{\rho u^2}{2p^2} - 2\frac{Y}{\rho} \\ -(\gamma-1)\frac{\rho u^3}{2p^2} & \frac{1}{p} + (\gamma-1)\frac{\rho u^2}{p^2} & -(\gamma-1)\frac{\rho u}{p^2} & (\gamma-1)q\frac{\rho u}{p^2} \\ -\frac{1}{p} + (\gamma-1)\frac{\rho u^2}{2p^2} & -(\gamma-1)\frac{\rho u}{p^2} & (\gamma-1)\frac{\rho}{p^2} & -(\gamma-1)q\frac{\rho}{p^2} \\ q\frac{1}{p} - (\gamma-1)q\frac{\rho u^2}{2p^2} & (\gamma-1)q\frac{\rho u}{p^2} & -(\gamma-1)q\frac{\rho}{p^2} & (\gamma-1)q^2\frac{\rho}{p^2} \end{vmatrix} \\ &+ \begin{vmatrix} \frac{\gamma}{\gamma-1}\frac{1}{\rho} + (\gamma-1)\frac{\rho u^4}{4p^2} + 2\frac{Y^2}{\rho} & -(\gamma-1)\frac{\rho u^3}{2p^2} & -\frac{1}{p} + (\gamma-1)\frac{\rho u^2}{2p^2} & q\frac{1}{p} - (\gamma-1)q\frac{\rho u^2}{2p^2} - 2\frac{Y}{\rho} \\ -(\gamma-1)\frac{\rho u^3}{2p^2} & \frac{1}{p} + (\gamma-1)\frac{\rho u^2}{p^2} & -(\gamma-1)\frac{\rho u}{p^2} & (\gamma-1)q\frac{\rho u}{p^2} \\ -\frac{1}{p} + (\gamma-1)\frac{\rho u^2}{2p^2} & -(\gamma-1)\frac{\rho u}{p^2} & (\gamma-1)\frac{\rho}{p^2} & -(\gamma-1)q\frac{\rho}{p^2} \\ -2\frac{Y}{\rho} & 0 & 0 & \frac{2}{\rho} \end{vmatrix} \\ &= \begin{vmatrix} \frac{\gamma}{\gamma-1}\frac{1}{\rho} + (\gamma-1)\frac{\rho u^4}{4p^2} + 2\frac{Y^2}{\rho} & -(\gamma-1)\frac{\rho u^3}{2p^2} & -\frac{1}{p} + (\gamma-1)\frac{\rho u^2}{2p^2} & q\frac{1}{p} - (\gamma-1)q\frac{\rho u^2}{2p^2} - 2\frac{Y}{\rho} \\ -(\gamma-1)\frac{\rho u^3}{2p^2} & \frac{1}{p} + (\gamma-1)\frac{\rho u^2}{p^2} & -(\gamma-1)\frac{\rho u}{p^2} & (\gamma-1)q\frac{\rho u}{p^2} \\ -\frac{1}{p} + (\gamma-1)\frac{\rho u^2}{2p^2} & -(\gamma-1)\frac{\rho u}{p^2} & (\gamma-1)\frac{\rho}{p^2} & -(\gamma-1)q\frac{\rho}{p^2} \\ -2\frac{Y}{\rho} & 0 & 0 & \frac{2}{\rho} \end{vmatrix} \\ &= 2\frac{Y}{\rho} \begin{vmatrix} -(\gamma-1)\frac{\rho u^3}{2p^2} & -\frac{1}{p} + (\gamma-1)\frac{\rho u^2}{2p^2} & q\frac{1}{p} - (\gamma-1)q\frac{\rho u^2}{2p^2} - 2\frac{Y}{\rho} \\ \frac{1}{p} + (\gamma-1)\frac{\rho u^2}{p^2} & -(\gamma-1)\frac{\rho u}{p^2} & (\gamma-1)q\frac{\rho u}{p^2} \\ -(\gamma-1)\frac{\rho u}{p^2} & (\gamma-1)\frac{\rho}{p^2} & -(\gamma-1)q\frac{\rho}{p^2} \end{vmatrix} + \frac{2}{\rho}|\mathsf{A}_3|. \end{aligned}$$

Furthermore, we have

$$
\begin{aligned}
2\frac{Y}{\rho}&\begin{vmatrix} -(\gamma-1)\frac{\rho u^3}{2p^2} & -\frac{1}{p}+(\gamma-1)\frac{\rho u^2}{2p^2} & q\frac{1}{p}-(\gamma-1)q\frac{\rho u^2}{2p^2}-2\frac{Y}{\rho} \\ \frac{1}{p}+(\gamma-1)\frac{\rho u^2}{p^2} & -(\gamma-1)\frac{\rho u}{p^2} & (\gamma-1)q\frac{\rho u}{p^2} \\ -(\gamma-1)\frac{\rho u}{p^2} & (\gamma-1)\frac{\rho}{p^2} & -(\gamma-1)q\frac{\rho}{p^2} \end{vmatrix} \\
&= 2\frac{Y}{\rho}\begin{vmatrix} -(\gamma-1)\frac{\rho u^3}{2p^2} & -\frac{1}{p}+(\gamma-1)\frac{\rho u^2}{2p^2} & q\frac{1}{p}-(\gamma-1)q\frac{\rho u^2}{2p^2} \\ \frac{1}{p}+(\gamma-1)\frac{\rho u^2}{p^2} & -(\gamma-1)\frac{\rho u}{p^2} & (\gamma-1)q\frac{\rho u}{p^2} \\ -(\gamma-1)\frac{\rho u}{p^2} & (\gamma-1)\frac{\rho}{p^2} & -(\gamma-1)q\frac{\rho}{p^2} \end{vmatrix} \\
&+ 2\frac{Y}{\rho}\begin{vmatrix} -(\gamma-1)\frac{\rho u^3}{2p^2} & -\frac{1}{p}+(\gamma-1)\frac{\rho u^2}{2p^2} & -2\frac{Y}{\rho} \\ \frac{1}{p}+(\gamma-1)\frac{\rho u^2}{p^2} & -(\gamma-1)\frac{\rho u}{p^2} & 0 \\ -(\gamma-1)\frac{\rho u}{p^2} & (\gamma-1)\frac{\rho}{p^2} & 0 \end{vmatrix} \\
&= -4\frac{Y^2}{\rho^2}\begin{vmatrix} \frac{1}{p}+(\gamma-1)\frac{\rho u^2}{p^2} & -(\gamma-1)\frac{\rho u}{p^2} \\ -(\gamma-1)\frac{\rho u}{p^2} & (\gamma-1)\frac{\rho}{p^2} \end{vmatrix}
\end{aligned}
$$

and

$$
\begin{aligned}
\frac{2}{\rho}|\mathsf{A}_3| &= \frac{2}{\rho}|\mathsf{A}_{\text{Euler}}| + \frac{2}{\rho}\begin{vmatrix} 2\frac{Y^2}{\rho} & -(\gamma-1)\frac{\rho u^3}{2p^2} & -\frac{1}{p}+(\gamma-1)\frac{\rho u^2}{2p^2} \\ 0 & \frac{1}{p}+(\gamma-1)\frac{\rho u^2}{p^2} & -(\gamma-1)\frac{\rho u}{p^2} \\ 0 & -(\gamma-1)\frac{\rho u}{p^2} & (\gamma-1)\frac{\rho}{p^2} \end{vmatrix} \\
&= \frac{2}{\rho}|\mathsf{A}_{\text{Euler}}| + 4\frac{Y^2}{\rho^2}\begin{vmatrix} \frac{1}{p}+(\gamma-1)\frac{\rho u^2}{p^2} & -(\gamma-1)\frac{\rho u}{p^2} \\ -(\gamma-1)\frac{\rho u}{p^2} & (\gamma-1)\frac{\rho}{p^2} \end{vmatrix}.
\end{aligned}
$$

Combining the above equations, we arrive at $|\eta_{UU}| = \frac{2}{\rho}|\mathsf{A}_{\text{Euler}}| > 0$. Therefore, all the leading principal minors of η_{UU} are positive and η_{UU} is positive definite. □

Remark 2.2. It will be seen in the next section that the strict convexity of the entropy function is crucial for constructing entropy stable schemes. More specifically, it will be used to formulate the Roe-type dissipation operator in terms of the entropy variables [28], which is not available if the entropy is not strictly convex.

Remark 2.3. According to the above analysis, for any $\ell > 0$, $\hat{\eta} + \ell\rho Y^2$ is also a strictly convex entropy and the corresponding entropy flux is $\hat{\phi} + \ell\rho u Y^2$.

Remark 2.4. It is direct to verify that U is orthogonal to the fourth column of η_{UU}. Then it follows that $U^T\eta_{UU}Q_U = (0,0,0,0)$ and thereby $U^T\eta_{UU}Q_U U = 0$. This relation may be helpful in the mathematical analysis of the reactive Euler equations.

2.2. **2D case.** The above entropy analysis can be directly extended to the 2D reactive Euler equations

$$\partial_t U + \partial_x F(U) + \partial_y G(U) = Q(U), \tag{2.8}$$

where

$$\begin{aligned}
&U = (\rho, \rho u, \rho v, \rho E, \rho Y)^T,\\
&F(U) = (\rho u, \rho u^2 + p, \rho uv, (\rho E + p)u, \rho uY)^T,\\
&G(U) = (\rho v, \rho uv, \rho v^2 + p, (\rho E + p)v, \rho vY)^T,\\
&Q(U) = (0, 0, 0, 0, \omega)
\end{aligned}$$

and $\rho E = \frac{1}{2}\rho(u^2 + v^2) + \frac{p}{\gamma-1} + q\rho Y$. Similar to the 1D case, $\eta = \hat{\eta} + \rho Y^2$, instead of the classical entropy function $\hat{\eta} = \frac{-\rho s}{\gamma-1}$, is a strictly convex entropy function for (2.8). The corresponding entropy fluxes are

$$\phi_1 = \hat{\phi}_1 + \rho u Y^2, \quad \phi_2 = \hat{\phi}_2 + \rho v Y^2, \tag{2.9}$$

where $\hat{\phi}_1 = \frac{-\rho us}{\gamma-1}, \hat{\phi}_2 = \frac{-\rho vs}{\gamma-1}$ are the classical entropy flux pair for the 2D Euler equations. It is direct to verify that

$$\partial_t \eta + \partial_x \phi_1 + \partial_y \phi_2 = (q\frac{\rho}{p} + 2Y)\omega \le 0 \tag{2.10}$$

and the entropy variables are

$$V := \eta_U = \begin{pmatrix} \frac{\gamma-s}{\gamma-1} - \frac{\rho(u^2+v^2)}{2p} - Y^2 \\ \frac{\rho u}{p} \\ \frac{\rho v}{p} \\ -\frac{\rho}{p} \\ q\frac{\rho}{p} + 2Y \end{pmatrix}. \tag{2.11}$$

The Hessian matrix of η is given by

(2.12)

$$\eta_{UU} = \begin{pmatrix} \frac{\gamma}{\gamma-1}\frac{1}{\rho} + (\gamma-1)\frac{\rho(u^2+v^2)^2}{4p^2} + 2\frac{Y^2}{\rho} & -(\gamma-1)\frac{\rho(u^2+v^2)u}{2p^2} & -(\gamma-1)\frac{\rho(u^2+v^2)v}{2p^2} \\ -(\gamma-1)\frac{\rho(u^2+v^2)u}{2p^2} & \frac{1}{p} + (\gamma-1)\frac{\rho u^2}{p^2} & (\gamma-1)\frac{\rho uv}{p^2} \\ -(\gamma-1)\frac{\rho(u^2+v^2)v}{2p^2} & (\gamma-1)\frac{\rho uv}{p^2} & \frac{1}{p} + (\gamma-1)\frac{\rho v^2}{p^2} \\ -\frac{1}{p} + (\gamma-1)\frac{\rho(u^2+v^2)}{2p^2} & -(\gamma-1)\frac{\rho u}{p^2} & -(\gamma-1)\frac{\rho v}{p^2} \\ q\frac{1}{p} - (\gamma-1)q\frac{\rho(u^2+v^2)}{2p^2} - 2\frac{Y}{\rho} & (\gamma-1)q\frac{\rho u}{p^2} & (\gamma-1)q\frac{\rho v}{p^2} \end{pmatrix}$$

$$\begin{pmatrix} -\frac{1}{p} + (\gamma-1)\frac{\rho(u^2+v^2)}{2p^2} & q\frac{1}{p} - (\gamma-1)q\frac{\rho(u^2+v^2)}{2p^2} - 2\frac{Y}{\rho} \\ -(\gamma-1)\frac{\rho u}{p^2} & (\gamma-1)q\frac{\rho u}{p^2} \\ -(\gamma-1)\frac{\rho v}{p^2} & (\gamma-1)q\frac{\rho v}{p^2} \\ (\gamma-1)\frac{\rho}{p^2} & -(\gamma-1)q\frac{\rho}{p^2} \\ -(\gamma-1)q\frac{\rho}{p^2} & (\gamma-1)q^2\frac{\rho}{p^2} + \frac{2}{\rho} \end{pmatrix},$$

which can be straightforwardly proved to be strictly convex as Theorem 2.1. The entropy potentials can be computed as $\psi_1 := V^T F - \phi_1 = \rho u$ and $\psi_2 := V^T G - \phi_2 = \rho v$.

3. Entropy stable schemes in 1D

Based on the strictly convex entropy above, in this section we construct second- and high-order finite difference entropy stable schemes within the framework of [31]. Here we consider 1D reactive Euler equations and the 2D case will be discussed in the next section.

We employ a uniform Cartesian mesh $\{x_i\}$ with mesh size $\Delta x = x_{i+1} - x_i$ and the point values are denoted as U_i. Set $x_{i+1/2} = \frac{1}{2}(x_{i+1} + x_i)$ and partition the domain into intervals $I_i = [x_{i-1/2}, x_{i+1/2}]$. A conservative finite difference method updating point values of the solution U for (2.1) has the form

$$\frac{d}{dt}U_i(t) = -\frac{1}{\Delta x}(\mathbf{F}_{i+1/2}(t) - \mathbf{F}_{i-1/2}(t)) + Q(U_i(t)), \tag{3.1}$$

where $\mathbf{F}_{i+1/2}$ is the numerical flux at the interface $x_{i+1/2}$.

Following [31], the scheme (3.1) is said to be entropy preserving[1] if it satisfies a discrete entropy equality

$$\frac{d}{dt}\eta(U_i(t)) = -\frac{1}{\Delta x}(\tilde{\phi}_{i+1/2} - \tilde{\phi}_{i-1/2}) + \eta_U(U_i(t))Q(U_i(t)) \tag{3.2}$$

for some numerical entropy flux $\tilde{\phi}_{i+1/2}$ consistent with ϕ. Denote by $V := \partial_U \eta$ the entropy variable and by $\psi(U) := V(U)^T F(U) - \phi(U)$ the entropy potential. With notations

$$[\![a]\!]_{i+1/2} = a_{i+1} - a_i, \quad \{\{a\}\}_{1/2} = \frac{1}{2}(a_{i+1} + a_i),$$

we have [31]

Theorem 3.1. *Assume that a consistent numerical flux $\tilde{\mathbf{F}}_{i+1/2}$ satisfies*

$$[\![V]\!]^T_{i+1/2}\tilde{\mathbf{F}}_{i+1/2} = [\![\psi]\!]_{i+1/2}. \tag{3.3}$$

Then the scheme with numerical flux $\tilde{\mathbf{F}}_{i+1/2}$ is second-order accurate and entropy preserving with the entropy flux given by

$$\tilde{\phi}_{i+1/2} = \{\{V\}\}^T_{i+1/2}\tilde{\mathbf{F}}_{i+1/2} - \{\{\psi\}\}_{i+1/2}. \tag{3.4}$$

Based on the entropy preserving numerical flux, an entropy stable scheme is built by adding appropriate dissipation terms as follows [31].

Theorem 3.2. *If the numerical flux of the scheme* (3.1) *is defined as*

$$\hat{\mathbf{F}}_{i+1/2} = \tilde{\mathbf{F}}_{i+1/2} - \frac{1}{2}\mathsf{D}_{i+1/2}[\![V]\!]_{i+1/2}, \tag{3.5}$$

where $\tilde{\mathbf{F}}_{i+1/2}$ satisfies the entropy preserving condition (3.3) *and $\mathsf{D}_{i+1/2}$ is a semi-positive definite matrix, then the scheme* (3.1) *is first-order accurate and satisfies*

(3.6)

$$\begin{aligned}
&\frac{d}{dt}\eta(U_i(t)) + \frac{1}{\Delta x}(\hat{\phi}_{i+1/2} - \hat{\phi}_{i-1/2}) \\
&= -\frac{1}{4\Delta x}([\![V]\!]^T_{i+1/2}\mathsf{D}_{i+1/2}[\![V]\!]_{i+1/2} + [\![V]\!]^T_{i-1/2}\mathsf{D}_{i-1/2}[\![V]\!]_{i-1/2}) + \eta_U(U_i(t))Q(U_i(t)) \\
&\le \eta_U(U_i(t))Q(U_i(t)) \le 0.
\end{aligned}$$

[1]Here we use "entropy preserving" instead of "entropy conservative" due to the source term in (2.5) or (3.2).

Here

$$\hat{\phi}_{i+1/2} = \tilde{\phi}_{i+1/2} - \frac{1}{2}\{\{V\}\}^T_{i+1/2}\mathsf{D}_{i+1/2}[\![V]\!]_{i+1/2} \tag{3.7}$$

and $\tilde{\phi}_{i+1/2}$ *is the entropy flux associated with* $\tilde{\mathbf{F}}_{i+1/2}$ *in* (3.4).

3.1. **Two-point entropy preserving flux.** In the following we derive two-point entropy preserving flux $\tilde{\mathbf{F}}_{i+1/2} = \tilde{\mathbf{F}}(U_i(t), U_{i+1}(t))$ that satisfies condition (3.3). To simplify notations, we drop the subscript $i+1/2$ and write (3.3) as

$$[\![V]\!]^T\tilde{\mathbf{F}} = [\![\psi]\!]. \tag{3.8}$$

Following [22, 28], we introduce the logarithmic average

$$\{\{a\}\}^{\ln} = \frac{[\![a]\!]}{[\![\ln(a)]\!]}$$

and have the identities

$$[\![ab]\!] = [\![a]\!]\{\{b\}\} + [\![b]\!]\{\{a\}\}, \quad [\![\ln(a)]\!] = [\![a]\!]/\{\{a\}\}^{\ln}.$$

With these, we construct two sets of entropy preserving flux by extending those in [5, 28] for the Euler equations.

Let $V = (V^1, V^2, V^3, V^4)^T$ and $\tilde{\mathbf{F}} = (\tilde{\mathbf{F}}^1, \tilde{\mathbf{F}}^2, \tilde{\mathbf{F}}^3, \tilde{\mathbf{F}}^4)^T$. Define a set of algebraic variables [22, 28]

$$z = \begin{pmatrix} z^1 \\ z^2 \\ z^3 \\ z^4 \end{pmatrix} = \sqrt{\frac{\rho}{p}} \begin{pmatrix} 1 \\ u \\ p \\ Y\sqrt{\frac{p}{\rho}} \end{pmatrix}. \tag{3.9}$$

Following the procedure in [22, 28], we write each jump term in (3.8) in terms of jumps of the algebraic variables:

$$\begin{aligned}
[\![V^1]\!] &= [\![\frac{\gamma - s}{\gamma - 1} - \frac{\rho u^2}{2p} - Y^2]\!] \\
&= [\![\frac{\gamma - \ln(\frac{z^3}{z^1}) + \gamma\ln(z^1 z^3)}{\gamma - 1} - \frac{1}{2}(z^2)^2 - (z^4)^2]\!] \\
&= \frac{\gamma + 1}{\gamma - 1}[\![\ln(z^1)]\!] + [\![\ln(z^3)]\!] - \frac{1}{2}[\![(z^2)^2]\!] - [\![(z^4)^2]\!] \\
&= \frac{\gamma + 1}{\gamma - 1}\frac{[\![z^1]\!]}{\{\{z^1\}\}^{\ln}} + \frac{[\![z^3]\!]}{\{\{z^3\}\}^{\ln}} - \{\{z^2\}\}[\![z^2]\!] - 2\{\{z^4\}\}[\![z^4]\!], \\
[\![V^2]\!] &= [\![\frac{\rho u}{p}]\!] = [\![z^1 z^2]\!] = \{\{z^2\}\}[\![z^1]\!] + \{\{z^1\}\}[\![z^2]\!], \\
[\![V^3]\!] &= [\![-\frac{\rho}{p}]\!] = [\![-(z^1)^2]\!] = -2\{\{z^1\}\}[\![z^1]\!], \\
[\![V^4]\!] &= [\![q\frac{\rho}{p} + 2Y]\!] = [\![-q(z^1)^2 + 2z^4]\!] = -2q\{\{z^1\}\}[\![z^1]\!] + 2[\![z^4]\!], \\
[\![\psi]\!] &= [\![z^2 z^3]\!] = \{\{z^3\}\}[\![z^2]\!] + \{\{z^2\}\}[\![z^3]\!],
\end{aligned}$$

where the identities above have been used. Substituting these expressions into (3.8) and matching the coefficients of $[\![z^l]\!], l = 1, 2, 3, 4$, we obtain a set of linear equations

with respect to $\tilde{\mathbf{F}}^l, l = 1, 2, 3, 4$:

$$\begin{aligned}
&\frac{\gamma+1}{\gamma-1}\frac{1}{\{\{z^1\}\}^{\ln}}\tilde{\mathbf{F}}^1 + \{\{z^2\}\}\tilde{\mathbf{F}}^2 - 2\{\{z^1\}\}\tilde{\mathbf{F}}^3 - 2q\{\{z^1\}\}\tilde{\mathbf{F}}^4 = 0,\\
&-\{\{z^2\}\}\tilde{\mathbf{F}}^1 + \{\{z^1\}\}\tilde{\mathbf{F}}^2 = \{\{z^3\}\},\\
&\frac{1}{\{\{z^3\}\}^{\ln}}\tilde{\mathbf{F}}^1 = \{\{z^2\}\},\\
&-2\{\{z^4\}\}\tilde{\mathbf{F}}^1 + 2\tilde{\mathbf{F}}^4 = 0.
\end{aligned}$$

Then $\tilde{\mathbf{F}}^l$ can be solved out as

$$\begin{aligned}
\tilde{\mathbf{F}}^1 &= \{\{z^2\}\}\{\{z^3\}\}^{\ln},\\
\tilde{\mathbf{F}}^2 &= \frac{\{\{z^3\}\}}{\{\{z^1\}\}} + \frac{\{\{z^2\}\}}{\{\{z^1\}\}}\tilde{\mathbf{F}}^1,\\
\tilde{\mathbf{F}}^3 &= \frac{1}{2}\frac{\gamma+1}{\gamma-1}\frac{1}{\{\{z^1\}\}\{\{z^1\}\}^{\ln}}\tilde{\mathbf{F}}^1 + \frac{1}{2}\frac{\{\{z^2\}\}}{\{\{z^1\}\}}\tilde{\mathbf{F}}^2 + q\tilde{\mathbf{F}}^4,\\
\tilde{\mathbf{F}}^4 &= \{\{z^4\}\}\tilde{\mathbf{F}}^1.
\end{aligned} \tag{3.10}$$

It is easy to see that this set of numerical flux, satisfying the entropy preserving condition (3.8), is consistent with $F(U)$ in (2.1). When $\tilde{\mathbf{F}}^4 = 0$, $\tilde{\mathbf{F}}^l, l = 1, 2, 3$ degenerate to those for the Euler equations in [22, 28].

Next we construct another set of entropy preserving flux by defining the algebraic variables as [5]

$$z = \begin{pmatrix} z^1 \\ z^2 \\ z^3 \\ z^4 \end{pmatrix} = \begin{pmatrix} \rho \\ u \\ \frac{\rho}{p} \\ Y \end{pmatrix}. \tag{3.11}$$

With the same procedure above, we use these algebraic variables to derive the following entropy preserving flux:

$$\begin{aligned}
\tilde{\mathbf{F}}^1 &= \{\{z^1\}\}^{\ln}\{\{z^2\}\},\\
\tilde{\mathbf{F}}^2 &= \frac{\{\{z^1\}\}}{\{\{z^3\}\}} + \{\{z^2\}\}\tilde{\mathbf{F}}^1,\\
\tilde{\mathbf{F}}^3 &= \left(\frac{1}{(\gamma-1)\{\{z^3\}\}^{\ln}} - \frac{1}{2}\{\{(z^2)^2\}\}\right)\tilde{\mathbf{F}}^1 + \{\{z^2\}\}\tilde{\mathbf{F}}^2 + q\tilde{\mathbf{F}}^4,\\
\tilde{\mathbf{F}}^4 &= \{\{z^4\}\}\tilde{\mathbf{F}}^1.
\end{aligned} \tag{3.12}$$

When $\tilde{\mathbf{F}}^4 = 0$, $\tilde{\mathbf{F}}^l, l = 1, 2, 3$ degenerate to those for the Euler equations in [5]. Except for the preserving of entropy, an additional property of this set of flux is that it is kinetic-energy preserving (KEP) in the sense of Jameson [23], which is useful in turbulent flow simulations [30]. Specifically, note that the momentum flux $\tilde{\mathbf{F}}^2$ can be written as $\tilde{\mathbf{F}}^2 = \tilde{p} + \{\{u\}\}\tilde{\mathbf{F}}^1$, where $\tilde{p} := \frac{\{\{z^1\}\}}{\{\{z^3\}\}}$ is a consistent pressure

average. With this, we have

$$\begin{aligned}\sum_i \Delta x \frac{d(\frac{1}{2}\rho u^2)_i}{dt} &= \sum_i \Delta x \left[-\frac{1}{2}u_i^2\frac{d\rho_i}{dt} + u_i\frac{d(\rho u)_i}{dt}\right] \\ &= \sum_i \Delta x \left[\frac{1}{2}u_i^2(\tilde{\mathbf{F}}^1_{i+1/2} - \tilde{\mathbf{F}}^1_{i-1/2}) - u_i(\tilde{\mathbf{F}}^2_{i+1/2} - \tilde{\mathbf{F}}^2_{i-1/2})\right] \\ &= \sum_i \Delta x \left[\frac{1}{2}(u_i^2 - u_{i+1}^2)\tilde{\mathbf{F}}^1_{i+1/2} - (u_i - u_{i+1})\tilde{\mathbf{F}}^2_{i+1/2}\right] \\ &= \sum_i \Delta x (u_{i+1} - u_i)\tilde{p}_{i+1/2},\end{aligned}$$

which is consistent with the kinetic energy equation $\frac{d}{dt}\int \frac{1}{2}\rho u^2 dx = \int p\frac{\partial u}{\partial x}dx$. In this sense, the flux (3.12) is KEP.

3.2. **Dissipation matrix.** Although Theorem 3.2 holds for any semi-positive definite $\mathsf{D}_{j+1/2}$, a popular choice is to recast Roe's dissipation term $\mathsf{R}|\Lambda|\mathsf{R}^{-1}[\![U]\!]$ to $\mathsf{D}[\![V]\!]$ in terms of the entropy variable, where R is the matrix of eigenvectors of the flux Jacobian $\partial_U F$ and $|\Lambda| = \mathrm{diag}(|\lambda_1|, |\lambda_2|, \ldots, |\lambda_M|)$ with λ_i the eigenvalues of $\partial_U F$.

Denote $\mathsf{A} = \partial_U F$ and note that $\eta_{UU}\mathsf{A}$ is symmetric as η is strictly convex. Assume that we have already obtained a complete set of (row) eigenvectors $\tilde{\mathsf{L}}$ such that $\mathsf{A} = \tilde{\mathsf{L}}^{-1}\Lambda\tilde{\mathsf{L}}$, where $\Lambda = \mathrm{diag}(\lambda_1, \lambda_2, \ldots, \lambda_M)$ and λ_i are the eigenvalues of A. Thanks to the strict convexity of the entropy, i.e., η_{UU} is positive definite, there exists a symmetric block diagonal matrix G that block scales the eigenvectors $\tilde{\mathsf{L}}$ in such a manner that (see Barth's eigenscaling theorem in [2])

$$\mathsf{A} = (\mathsf{G}\tilde{\mathsf{L}})^{-1}\Lambda(\mathsf{G}\tilde{\mathsf{L}}), \quad \eta_{UU} = (\mathsf{G}\tilde{\mathsf{L}})^T(\mathsf{G}\tilde{\mathsf{L}}).$$

The dimensions of the blocks of G correspond to the multiplicities of the eigenvalues λ_i. It follows from the above equation that $\mathsf{G} = (\tilde{\mathsf{L}}^{-T}\eta_{UU}\tilde{\mathsf{L}}^{-1})^{\frac{1}{2}}$, which can be easily obtained without directly computing η_{UU}^{-1} since $\mathsf{G}^2 = \tilde{\mathsf{L}}^{-T}\eta_{UU}\tilde{\mathsf{L}}^{-1}$ is block diagonal.

With the above $\tilde{\mathsf{L}}$ and G, we define $\mathsf{R} = (\mathsf{G}\tilde{\mathsf{L}})^{-1} = \tilde{\mathsf{L}}^{-1}\mathsf{G}^{-1}$ and then

$$\mathsf{A} = \mathsf{R}\Lambda\mathsf{R}^{-1}, \quad \eta_{UU} = \mathsf{R}^{-T}\mathsf{R}^{-1}. \tag{3.13}$$

Thus we have

$$\mathsf{R}|\Lambda|\mathsf{R}^{-1}\mathrm{d}U = \mathsf{R}|\Lambda|\mathsf{R}^{-1}\eta_{UU}^{-1}\mathrm{d}V = \mathsf{R}|\Lambda|\mathsf{R}^T\mathrm{d}V$$

and Roe's dissipation term in terms of the entropy variable is

$$\mathsf{D}[\![V]\!], \quad \mathsf{D} = \mathsf{R}|\Lambda|\mathsf{R}^T.$$

If $|\Lambda|$ is replaced by $\max\{|\lambda_1|, |\lambda_2|, \ldots, |\lambda_M|\}\mathsf{I}$ with I the unit matrix, then we obtain the Rusanov-type dissipation term

$$\mathsf{D}[\![V]\!], \quad \mathsf{D} = \max\{|\lambda_1|, |\lambda_2|, \ldots, |\lambda_M|\}\mathsf{R}\mathsf{R}^T = \max\{|\lambda_1|, |\lambda_2|, \ldots, |\lambda_M|\}\eta_{UU}^{-1}.$$

The key step of constructing the above dissipation terms is to compute the eigenvector matrix R satisfying (3.13). In the following we derive such R for the reactive Euler equations (2.1). Let $H = E + \frac{p}{\rho} = \frac{\gamma}{\gamma-1}\frac{p}{\rho} + \frac{1}{2}u^2 + qY$ and $c = \sqrt{\gamma\frac{p}{\rho}}$.

The flux Jacobian $\mathsf{A} = \partial_U \mathbf{F}$ of the reactive Euler equations (2.1) can be computed as

$$\mathsf{A} = \begin{pmatrix} 0 & 1 & 0 & 0 \\ \frac{\gamma-3}{2}u^2 & (3-\gamma)u & \gamma-1 & -(\gamma-1)q \\ \frac{\gamma-1}{2}u^3 - Hu & H-(\gamma-1)u^2 & \gamma u & -(\gamma-1)qu \\ -uY & Y & 0 & u \end{pmatrix},$$

the eigenvalues of which are $u, u, u+c$ and $u-c$. Based on the widely used eigensystem (see e.g. [24]) for the Euler equations, we obtain the following left and right eigenvectors of A:

$$\tilde{\mathsf{L}} = \begin{pmatrix} 1-\frac{\gamma-1}{2}\frac{u^2}{c^2} & (\gamma-1)\frac{u}{c^2} & -\frac{\gamma-1}{c^2} & q\frac{\gamma-1}{c^2} \\ -\frac{\gamma-1}{2}\frac{u^2}{c^2}Y & (\gamma-1)\frac{u}{c^2}Y & -\frac{\gamma-1}{c^2}Y & 1+q\frac{\gamma-1}{c^2} \\ \frac{\gamma-1}{4}\frac{u^2}{c^2} - \frac{1}{2}\frac{u}{c} & -\frac{\gamma-1}{2}\frac{u}{c^2} + \frac{1}{2c} & \frac{\gamma-1}{2c^2} & -q\frac{\gamma-1}{2c^2} \\ \frac{\gamma-1}{4}\frac{u^2}{c^2} + \frac{1}{2}\frac{u}{c} & -\frac{\gamma-1}{2}\frac{u}{c^2} - \frac{1}{2c} & \frac{\gamma-1}{2c^2} & -q\frac{\gamma-1}{2c^2} \end{pmatrix}, \tag{3.14}$$

$$\tilde{\mathsf{R}} = \tilde{\mathsf{L}}^{-1} = \begin{pmatrix} 1 & 0 & 1 & 1 \\ u & 0 & u+c & u-c \\ \frac{1}{2}u^2 & q & H+uc & H-uc \\ 0 & 1 & Y & Y \end{pmatrix},$$

which satisfy $\tilde{\mathsf{L}}\mathsf{A}\tilde{\mathsf{R}} = \operatorname{diag}(u, u, u+c, u-c)$. It is direct to compute that

$$\mathsf{G}^2 = \tilde{\mathsf{L}}^{-T}\eta_{UU}\tilde{\mathsf{L}}^{-1} = \operatorname{diag}(\mathsf{C}, \frac{2\gamma}{\rho}, \frac{2\gamma}{\rho}), \quad \mathsf{C} = \begin{pmatrix} \frac{\gamma}{\gamma-1}\frac{1}{\rho} + 2\frac{Y^2}{\rho} & -2\frac{Y}{\rho} \\ -2\frac{Y}{\rho} & \frac{2}{\rho} \end{pmatrix}.$$

The 2×2 matrix C can be diagonalized as $\mathsf{C} = \mathsf{M}\operatorname{diag}(\zeta_1, \zeta_2)\mathsf{M}^T$, where $\zeta_1, \zeta_2 = \frac{1}{\rho}(\frac{3\gamma-2}{2\gamma-2} + Y^2) \pm \frac{1}{\rho}\sqrt{(\frac{3\gamma-2}{2\gamma-2}+Y^2)^2 - \frac{2\gamma}{\gamma-1}}$ and M is a unitary matrix given by

$$\mathsf{M} = \begin{pmatrix} \frac{\zeta_1\rho-2}{\sqrt{(\zeta_1\rho-2)^2+4Y^2}} & \frac{\zeta_2\rho-2}{\sqrt{(\zeta_2\rho-2)^2+4Y^2}} \\ \frac{2Y}{\sqrt{(\zeta_1\rho-2)^2+4Y^2}} & \frac{2Y}{\sqrt{(\zeta_2\rho-2)^2+4Y^2}} \end{pmatrix}.$$

Then we have

$$\mathsf{C}^{-\frac{1}{2}} := \begin{pmatrix} g_1 & g_2 \\ g_2 & g_3 \end{pmatrix} = \mathsf{M}\operatorname{diag}(\frac{1}{\sqrt{\zeta_1}}, \frac{1}{\sqrt{\zeta_2}})\mathsf{M}^T$$

and

$$\mathsf{R} = \tilde{\mathsf{R}}\mathsf{G}^{-1} = \begin{pmatrix} g_1 & g_2 & \sqrt{\frac{\rho}{2\gamma}} & \sqrt{\frac{\rho}{2\gamma}} \\ ug_1 & ug_2 & (u+c)\sqrt{\frac{\rho}{2\gamma}} & (u-c)\sqrt{\frac{\rho}{2\gamma}} \\ \frac{1}{2}u^2g_1 + qg_2 & \frac{1}{2}u^2g_2 + qg_3 & (H+uc)\sqrt{\frac{\rho}{2\gamma}} & (H-uc)\sqrt{\frac{\rho}{2\gamma}} \\ g_2 & g_3 & Y\sqrt{\frac{\rho}{2\gamma}} & Y\sqrt{\frac{\rho}{2\gamma}} \end{pmatrix}, \quad \eta_{UU}^{-1} = \mathsf{R}\mathsf{R}^T,$$

with which the dissipation matrix D and the dissipation term can be computed.

3.3. **High-order entropy stable schemes.** The semi-discrete entropy preserving scheme with the two-point flux $\tilde{\mathbf{F}}_{i+1/2}$ is only second-order accurate, while the entropy stable scheme with flux $\hat{\mathbf{F}}_{i+1/2}$ is only first-order accurate due to the dissipation term. In this subsection high-order entropy preserving/stable fluxes are constructed based on the two-point fluxes following [16, 25].

3.3.1. *High-order entropy preserving flux.* The high-order entropy preserving flux is defined as a linear combination of two-point fluxes [25]:

$$\tilde{\mathbf{F}}^{2k}_{i+1/2} = \sum_{r=1}^{k} \alpha_{k,r} \sum_{s=0}^{r-1} \tilde{\mathbf{F}}(U_{i-s}, U_{i-s+r}) \tag{3.15}$$

with constants $\alpha_{k,r}$ satisfying

$$\sum_{r=1}^{k} r\alpha_{k,r} = 1, \quad \sum_{r=1}^{k} r^{2s-1}\alpha_{k,r} = 0, \quad s = 2, \dots, k. \tag{3.16}$$

For example, the fourth- and sixth-order fluxes are

$$\begin{aligned}
\tilde{\mathbf{F}}^{4}_{i+1/2} &= \frac{4}{3}\tilde{\mathbf{F}}(U_i, U_{i+1}) - \frac{1}{6}(\tilde{\mathbf{F}}(U_{i-1}, U_{i+1}) + \tilde{\mathbf{F}}(U_i, U_{i+2})),\\
\tilde{\mathbf{F}}^{6}_{i+1/2} &= \frac{3}{2}\tilde{\mathbf{F}}(U_i, U_{i+1}) - \frac{3}{10}(\tilde{\mathbf{F}}(U_{i-1}, U_{i+1}) + \tilde{\mathbf{F}}(U_i, U_{i+2}))\\
&\quad + \frac{1}{30}(\tilde{\mathbf{F}}(U_{i-2}, U_{i+1}) + \tilde{\mathbf{F}}(U_{i-1}, U_{i+2}) + \tilde{\mathbf{F}}(U_i, U_{i+3})).
\end{aligned}$$

It is direst to see the consistence of the flux (3.15) by using the first condition in (3.16). Additionally, under the conditions (3.16), the scheme with flux (3.15) has $2k$-th order accuracy [25].

We show the entropy preserving property by computing

$$\begin{aligned}
&V_i^T(\tilde{\mathbf{F}}^{2k}_{i+1/2} - \tilde{\mathbf{F}}^{2k}_{i-1/2}) = \sum_{r=1}^{k} \alpha_{k,r} V_i^T(\tilde{\mathbf{F}}(U_i, U_{i+r}) - \tilde{\mathbf{F}}(U_{i-r}, U_i))\\
&= \sum_{r=1}^{k} \alpha_{k,r} \left[\left(\frac{V_i + V_{i+r}}{2} - \frac{V_{i+r} - V_i}{2} \right)^T \tilde{\mathbf{F}}(U_i, U_{i+r}) - \left(\frac{V_i + V_{i-r}}{2} + \frac{V_i - V_{i-r}}{2} \right)^T \tilde{\mathbf{F}}(U_{i-r}, U_i) \right]\\
&= \sum_{r=1}^{k} \alpha_{k,r} \left[\frac{V_i + V_{i+r}}{2} \cdot \tilde{\mathbf{F}}(U_i, U_{i+r}) - \frac{1}{2}[\![\psi]\!]_{i+r,i} - \frac{V_i + V_{i-r}}{2} \cdot \tilde{\mathbf{F}}(U_{i-r}, U_i) - \frac{1}{2}[\![\psi]\!]_{i,i-r} \right]\\
&= \sum_{r=1}^{k} \alpha_{k,r} \left[\left(\frac{V_i + V_{i+r}}{2} \cdot \tilde{\mathbf{F}}(U_i, U_{i+r}) - \{\{\psi\}\}_{i+r,i} \right) - \left(\frac{V_i + V_{i-r}}{2} \cdot \tilde{\mathbf{F}}(U_{i-r}, U_i) - \{\{\psi\}\}_{i,i-r} \right) \right].
\end{aligned}$$

Thus the discrete entropy flux is

$$\tilde{\phi}^{2k}_{i+1/2} = \sum_{r=1}^{k} \alpha_{k,r} \left(\frac{V_i + V_{i+r}}{2} \cdot \tilde{\mathbf{F}}(U_i, U_{i+r}) - \{\{\psi\}\}_{i+r,i} \right) \tag{3.17}$$

and the scheme is entropy preserving with the discrete entropy equality given by

$$\frac{d}{dt}\eta(U_i(t)) = -\frac{1}{\Delta x}(\tilde{\phi}^{2k}_{i+1/2} - \tilde{\phi}^{2k}_{i-1/2}) + \eta_U(U_i(t))Q(U_i(t)).$$

3.3.2. *High-order entropy stable flux.* With the high-order entropy preserving flux above, we follow [16] to construct high-order entropy stable fluxes by adding high-order dissipation terms based on ENO and WENO reconstructions. The high-order entropy stable flux based on ENO is defined as [16]

$$\hat{\mathbf{F}}_{i+1/2} = \tilde{\mathbf{F}}^{2k}_{i+1/2} - \frac{1}{2}\mathsf{R}_{i+1/2}|\Lambda_{i+1/2}| \ll \omega \gg^{ENO}_{i+1/2} \tag{3.18}$$

with $\tilde{\mathbf{F}}^{2k}_{i+1/2}$ the $2k$-th order entropy preserving flux in (3.15) and $\ll \omega \gg^{ENO}_{i+1/2} := \omega^+_{i+1/2} - \omega^-_{i+1/2}$. Here $\omega^+_{i+1/2}$ and $\omega^-_{i+1/2}$ are the right and left limiting values of the scaled entropy variables $\omega := \mathsf{R}^T_{i+1/2}V$ at the interface $x_{i+1/2}$, respectively, and

they are obtained by $2k$-th order ENO reconstruction. It is shown in [17] that the ENO reconstruction satisfies the sign property

$$\operatorname{sign}(\ll \omega \gg^{ENO}_{i+1/2}) = \operatorname{sign}(\llbracket \omega \rrbracket_{i+1/2}). \tag{3.19}$$

With this, the entropy stable property of the ENO based flux (3.18) can be shown by computing

$$\begin{aligned}
&V_i^T(\hat{\mathbf{F}}_{i+1/2} - \hat{\mathbf{F}}_{i-1/2}) \\
&= V_i^T(\tilde{\mathbf{F}}^{2k}_{i+1/2} - \tilde{\mathbf{F}}^{2k}_{i-1/2}) \\
&- \frac{1}{2} V_i^T \mathsf{R}_{i+1/2} |\Lambda_{i+1/2}| \ll \omega \gg^{ENO}_{i+1/2} + \frac{1}{2} V_i^T \mathsf{R}_{i-1/2} |\Lambda_{i-1/2}| \ll \omega \gg^{ENO}_{i-1/2} \\
&= \tilde{\phi}^{2k}_{i+1/2} - \tilde{\phi}^{2k}_{i-1/2} - \frac{1}{2}(\{\{V\}\}_{i+1/2} - \frac{1}{2}\llbracket V \rrbracket_{i+1/2})^T R_{i+1/2} |\Lambda_{i+1/2}| \ll \omega \gg^{ENO}_{i+1/2} \\
&+ \frac{1}{2}(\{\{V\}\}_{i-1/2} + \frac{1}{2}\llbracket V \rrbracket_{i+1/2})^T R_{i-1/2} |\Lambda_{i-1/2}| \ll \omega \gg^{ENO}_{i-1/2} \\
&= \left(\tilde{\phi}^{2k}_{i+1/2} - \frac{1}{2}\{\{V\}\}^T_{i+1/2} R_{i+1/2} |\Lambda_{i+1/2}| \ll \omega \gg^{ENO}_{i+1/2} \right) \\
&- \left(\tilde{\phi}^{2k}_{i-1/2} - \frac{1}{2}\{\{V\}\}^T_{i-1/2} R_{i-1/2} |\Lambda_{i-1/2}| \ll \omega \gg^{ENO}_{i-1/2} \right) \\
&+ \frac{1}{4} \Big(\llbracket V \rrbracket^T_{i+1/2} R_{i+1/2} |\Lambda_{i+1/2}| \ll \omega \gg^{ENO}_{i+1/2} \\
&\qquad + \{\{V\}\}^T_{i-1/2} R_{i-1/2} |\Lambda_{i-1/2}| \ll \omega \gg^{ENO}_{i-1/2} \Big) \\
&= \hat{\phi}^{ENO}_{i+1/2} - \hat{\phi}^{ENO}_{i-1/2} + \frac{1}{4} \Big(\llbracket \omega \rrbracket^T_{i+1/2} |\Lambda_{i+1/2}| \ll \omega \gg^{ENO}_{i+1/2} \\
&\qquad + \llbracket \omega \rrbracket^T_{i-1/2} |\Lambda_{i-1/2}| \ll \omega \gg^{ENO}_{i-1/2} \Big),
\end{aligned}$$

where

$$\hat{\phi}^{ENO}_{i+1/2} = \tilde{\phi}^{2k}_{i+1/2} - \frac{1}{2}\{\{V\}\}^T_{i+1/2} R_{i+1/2} |\Lambda_{i+1/2}| \ll \omega \gg^{ENO}_{i+1/2}.$$

Thus we arrive at

$$\begin{aligned}
&\frac{\mathrm{d}\eta(U_i)}{\mathrm{d}t} + \frac{\hat{\phi}^{ENO}_{i+1/2} - \hat{\phi}^{ENO}_{i-1/2}}{\Delta x} \\
&= -\frac{1}{4\Delta x} \left(\llbracket \omega \rrbracket^T_{i+1/2} |\Lambda_{i+1/2}| \ll \omega \gg^{ENO}_{i+1/2} + \llbracket \omega \rrbracket^T_{i-1/2} |\Lambda_{i-1/2}| \ll \omega \gg^{ENO}_{i-1/2} \right) \\
&\quad + V_i^T Q(U_i(t)) \\
&\le V_i^T Q(U_i(t)) \le 0,
\end{aligned}$$

where $-\frac{1}{4\Delta x} \left(\llbracket \omega \rrbracket^T_{i+1/2} |\Lambda_{i+1/2}| \ll \omega \gg^{ENO}_{i+1/2} + \llbracket \omega \rrbracket^T_{i-1/2} |\Lambda_{i-1/2}| \ll \omega \gg^{ENO}_{i-1/2} \right) \le 0$ thanks to the sign property (3.19). This indicates that the flux (3.18) guarantees the entropy stable property.

The WENO based high-order entropy stable flux is defined as [3]

$$\hat{\mathbf{F}}_{i+1/2} = \tilde{\mathbf{F}}^{2k}_{i+1/2} - \frac{1}{2}\mathsf{R}_{i+1/2}|\Lambda_{i+1/2}| \ll \omega \gg^{WENO}_{i+1/2}, \tag{3.20}$$

where the l-th component of the $\ll \omega \gg^{WENO}_{i+1/2}$ is given by

$$\begin{aligned} &\ll \omega_l \gg^{WENO}_{i+1/2} = \theta_{l,i+1/2}(\omega^+_{l,i+1/2} - \omega^-_{l,i+1/2}),\\ &\theta_{l,i+1/2} := \begin{cases} 1, & (\omega^+_{l,i+1/2} - \omega^-_{l,i+1/2})[\![\omega_l]\!]_{i+1/2} > 0,\\ 0, & \text{otherwise.} \end{cases} \end{aligned} \tag{3.21}$$

Here $\omega^+_{l,i+1/2}$ and $\omega^-_{l,i+1/2}$ denote, respectively, the right and left limiting values of ω_l at the interface $x_{i+1/2}$ by using the $(2k-1)$-th order WENO reconstruction. Though the standard WENO reconstruction may not satisfy the sign property, the switch operator $\theta_{l,i+1/2}$ ensures that

$$\operatorname{sign}(\ll \omega \gg^{WENO}_{l,i+1/2}) = \operatorname{sign}([\![\omega]\!]_{l,i+1/2}). \tag{3.22}$$

With this relation, the entropy stable property can be proved in the same way as for the ENO based flux.

4. Entropy stable schemes in 2D

In this section, we construct entropy preserving/stable schemes for the 2D reactive Euler equations (2.8). The construction is similar to the 1D case and the key is to derive the two-point entropy preserving flux and the matrix R in the dissipation term.

4.1. **Two-point entropy preserving flux.**

As for the 1D case, here we propose two sets of entropy preserving fluxes satisfying

$$[\![V]\!]^T_{i+1/2,j}\tilde{\mathbf{F}}_{i+1/2,j} = [\![\psi_1]\!]_{i+1/2,j}, \quad [\![V]\!]^T_{i,j+1/2}\tilde{\mathbf{G}}_{i,j+1/2} = [\![\psi_2]\!]_{i,j+1/2}, \tag{4.1}$$

where $\tilde{\mathbf{F}}_{i+1/2,j}$ and $\tilde{\mathbf{G}}_{i,j+1/2}$ are numerical fluxes consistent with $F(U)$ and $G(U)$, respectively. Define algebraic variables

$$z = \begin{pmatrix} z^1\\ z^2\\ z^3\\ z^4\\ z^5 \end{pmatrix} = \sqrt{\frac{\rho}{p}}\begin{pmatrix} 1\\ u\\ v\\ p\\ Y \end{pmatrix}. \tag{4.2}$$

By writing each jump term in (4.1) in terms of jumps of the algebraic variables and matching the coefficients, we obtain

(4.3)

$$\tilde{\mathbf{F}}^1_{i+1/2,j} = \{\{z^2\}\}_{i+1/2,j}\{\{z^4\}\}^{\ln}_{i+1/2,j},$$

$$\tilde{\mathbf{F}}^2_{i+1/2,j} = \frac{\{\{z^4\}\}_{i+1/2,j}}{\{\{z^1\}\}_{i+1/2,j}} + \frac{\{\{z^2\}\}_{i+1/2,j}}{\{\{z^1\}\}_{i+1/2,j}}\tilde{\mathbf{F}}^1_{i+1/2,j},$$

$$\tilde{\mathbf{F}}^3_{i+1/2,j} = \frac{\{\{z^3\}\}_{i+1/2,j}}{\{\{z^1\}\}_{i+1/2,j}}\tilde{\mathbf{F}}^1_{i+1/2,j},$$

$$\tilde{\mathbf{F}}^4_{i+1/2,j} = \frac{1}{2}\frac{\gamma+1}{\gamma-1}\frac{1}{\{\{z^1\}\}_{i+1/2,j}\{\{z^1\}\}^{\ln}_{i+1/2,j}}\tilde{\mathbf{F}}^1_{i+1/2,j} + \frac{1}{2}\frac{\{\{z^2\}\}_{i+1/2,j}}{\{\{z^1\}\}_{i+1/2,j}}\tilde{\mathbf{F}}^2_{i+1/2,j}$$
$$+ \frac{1}{2}\frac{\{\{z^3\}\}_{i+1/2,j}}{\{\{z^1\}\}_{i+1/2,j}}\tilde{\mathbf{F}}^3_{i+1/2,j} + q\tilde{\mathbf{F}}^5_{i+1/2,j},$$

$$\tilde{\mathbf{F}}^5_{i+1/2,j} = \{\{\frac{z^5}{z^1}\}\}_{i+1/2,j}\tilde{\mathbf{F}}^1_{i+1/2,j},$$

$$\tilde{\mathbf{G}}^1_{i,j+1/2} = \{\{z^3\}\}_{i,j+1/2}\{\{z^4\}\}^{\ln}_{i,j+1/2},$$

$$\tilde{\mathbf{G}}^2_{i,j+1/2} = \frac{\{\{z^2\}\}_{i,j+1/2}}{\{\{z^1\}\}_{i,j+1/2}}\tilde{\mathbf{G}}^1_{i,j+1/2},$$

$$\tilde{\mathbf{G}}^3_{i,j+1/2} = \frac{\{\{z^4\}\}_{i,j+1/2}}{\{\{z^1\}\}_{i,j+1/2}} + \frac{\{\{z^3\}\}_{i,j+1/2}}{\{\{z^1\}\}_{i,j+1/2}}\tilde{\mathbf{G}}^1_{i,j+1/2},$$

$$\tilde{\mathbf{G}}^4_{i,j+1/2} = \frac{1}{2}\frac{\gamma+1}{\gamma-1}\frac{1}{\{\{z^1\}\}_{i,j+1/2}\{\{z^1\}\}^{\ln}_{i,j+1/2}}\tilde{\mathbf{G}}^1_{i,j+1/2} + \frac{1}{2}\frac{\{\{z^2\}\}_{i,j+1/2}}{\{\{z^1\}\}_{i,j+1/2}}\tilde{\mathbf{G}}^2_{i,j+1/2}$$
$$+ \frac{1}{2}\frac{\{\{z^3\}\}_{i,j+1/2}}{\{\{z^1\}\}_{i,j+1/2}}\tilde{\mathbf{G}}^3_{i,j+1/2} + q\tilde{\mathbf{G}}^5_{i,j+1/2},$$

$$\tilde{\mathbf{G}}^5_{i,j+1/2} = \{\{\frac{z^5}{z^1}\}\}_{i,j+1/2}\tilde{\mathbf{G}}^1_{i,j+1/2}.$$

On the other hand, if the algebraic variables are taken as

(4.4)
$$z = \begin{pmatrix} z^1 \\ z^2 \\ z^3 \\ z^4 \\ z^5 \end{pmatrix} = \begin{pmatrix} \rho \\ u \\ v \\ \frac{\rho}{p} \\ Y \end{pmatrix},$$

then the corresponding entropy preserving flux can be derived as

$$
\begin{aligned}
\tilde{\mathbf{F}}^1_{i+1/2,j} &= \{\{z^1\}\}^{\ln}_{i+1/2,j}\{\{z^2\}\}_{i+1/2,j},\\
\tilde{\mathbf{F}}^2_{i+1/2,j} &= \frac{\{\{z^1\}\}_{i+1/2,j}}{\{\{z^4\}\}_{i+1/2,j}} + \{\{z^2\}\}_{i+1/2,j}\tilde{\mathbf{F}}^1_{i+1/2,j},\\
\tilde{\mathbf{F}}^3_{i+1/2,j} &= \{\{z^3\}\}_{i+1/2,j}\tilde{\mathbf{F}}^1_{i+1/2,j},\\
\tilde{\mathbf{F}}^4_{i+1/2,j} &= \left(\frac{1}{(\gamma-1)\{\{z^4\}\}^{\ln}_{i+1/2,j}} - \frac{1}{2}\{\{(z^2)^2+(z^3)^2\}\}_{i+1/2,j}\right)\tilde{\mathbf{F}}^1_{i+1/2,j}\\
&\quad + \{\{z^2\}\}_{i+1/2,j}\tilde{\mathbf{F}}^2_{i+1/2,j} + \{\{z^3\}\}_{i+1/2,j}\tilde{\mathbf{F}}^3_{i+1/2,j} + q\tilde{\mathbf{F}}^5_{i+1/2,j},\\
\tilde{\mathbf{F}}^5_{i+1/2,j} &= \{\{z^5\}\}_{i+1/2,j}\tilde{\mathbf{F}}^1_{i+1/2,j},\\
\tilde{\mathbf{G}}^1_{i,j+1/2} &= \{\{z^1\}\}^{\ln}_{i,j+1/2}\{\{z^3\}\}_{i,j+1/2},\\
\tilde{\mathbf{G}}^2_{i,j+1/2} &= \{\{z^2\}\}_{i,j+1/2}\tilde{\mathbf{G}}^1_{i,j+1/2},\\
\tilde{\mathbf{G}}^3_{i,j+1/2} &= \frac{\{\{z^1\}\}_{i,j+1/2}}{\{\{z^4\}\}_{i,j+1/2}} + \{\{z^3\}\}_{i,j+1/2}\tilde{\mathbf{G}}^1_{i,j+1/2},\\
\tilde{\mathbf{G}}^4_{i,j+1/2} &= \left(\frac{1}{(\gamma-1)\{\{z^4\}\}^{\ln}_{i,j+1/2}} - \frac{1}{2}\{\{(z^2)^2+(z^3)^2\}\}_{i,j+1/2}\right)\tilde{\mathbf{G}}^1_{i,j+1/2}\\
&\quad + \{\{z^2\}\}_{i,j+1/2}\tilde{\mathbf{G}}^2_{i,j+1/2} + \{\{z^3\}\}_{i,j+1/2}\tilde{\mathbf{G}}^3_{i,j+1/2} + q\tilde{\mathbf{G}}^5_{i,j+1/2},\\
\tilde{\mathbf{G}}^5_{i,j+1/2} &= \{\{z^5\}\}_{i,j+1/2}\tilde{\mathbf{G}}^1_{i,j+1/2}.
\end{aligned}
\tag{4.5}
$$

Similar to the 1D case, this set of fluxes preserves both entropy and kinetic energy.

4.2. **Dissipation matrix.** Let $H = E + \frac{p}{\rho} = \frac{\gamma}{\gamma-1}\frac{p}{\rho} + \frac{1}{2}(u^2+v^2) + qY$ and $c = \sqrt{\gamma\frac{p}{\rho}}$. The flux Jacobian $\mathsf{A} = \partial_U F$ of the 2D reactive Euler equations (2.8) can be computed as

$$
\mathsf{A} = \begin{pmatrix}
0 & 1 & 0 & 0 & 0\\
\frac{\gamma-3}{2}u^2 + \frac{\gamma-1}{2}v^2 & (3-\gamma)u & (1-\gamma)v & \gamma-1 & -(\gamma-1)q\\
-uv & v & u & 0 & 0\\
\frac{\gamma-1}{2}(u^2+v^2)u - Hu & H-(\gamma-1)u^2 & -(\gamma-1)uv & \gamma u & -(\gamma-1)qu\\
-uY & Y & 0 & 0 & u
\end{pmatrix},
$$

the eigenvalues of which are $u, u, u, u+c$ and $u-c$. The left and right eigenvectors of A can be computed as

(4.6)

$$\tilde{\mathsf{L}}_A = \begin{pmatrix} 1-\frac{\gamma-1}{2}\frac{u^2+v^2}{c^2} & (\gamma-1)\frac{u}{c^2} & (\gamma-1)\frac{v}{c^2} & -\frac{\gamma-1}{c^2} & q\frac{\gamma-1}{c^2} \\ -v & 0 & 1 & 0 & 0 \\ -\frac{\gamma-1}{2}\frac{u^2+v^2}{c^2}Y & (\gamma-1)\frac{u}{c^2}Y & (\gamma-1)\frac{v}{c^2}Y & -\frac{\gamma-1}{c^2}Y & 1+q\frac{\gamma-1}{c^2}Y \\ \frac{\gamma-1}{4}\frac{u^2+v^2}{c^2}-\frac{1}{2}\frac{u}{c} & -\frac{\gamma-1}{2}\frac{u}{c^2}+\frac{1}{2c} & -\frac{\gamma-1}{2}\frac{v}{c^2} & \frac{\gamma-1}{2c^2} & -q\frac{\gamma-1}{2c^2} \\ \frac{\gamma-1}{4}\frac{u^2+v^2}{c^2}+\frac{1}{2}\frac{u}{c} & -\frac{\gamma-1}{2}\frac{u}{c^2}-\frac{1}{2c} & -\frac{\gamma-1}{2}\frac{v}{c^2} & \frac{\gamma-1}{2c^2} & -q\frac{\gamma-1}{2c^2} \end{pmatrix},$$

$$\tilde{\mathsf{R}}_A = \tilde{\mathsf{L}}_A^{-1} = \begin{pmatrix} 1 & 0 & 0 & 1 & 1 \\ u & 0 & 0 & u+c & u-c \\ v & 1 & 0 & v & v \\ \frac{1}{2}(u^2+v^2) & v & q & H+uc & H-uc \\ 0 & 0 & 1 & Y & Y \end{pmatrix},$$

which satisfy $\tilde{\mathsf{L}}_A\mathsf{A}\tilde{\mathsf{R}}_A = \mathrm{diag}(u, u, u, u+c, u-c)$.

The flux Jacobian $\mathsf{B} = \partial_U G$ is

$$\mathsf{B} = \begin{pmatrix} 0 & 0 & 1 & 0 & 0 \\ -uv & v & u & 0 & 0 \\ \frac{\gamma-3}{2}v^2+\frac{\gamma-1}{2}u^2 & (1-\gamma)u & (3-\gamma)v & \gamma-1 & -(\gamma-1)q \\ \frac{\gamma-1}{2}(u^2+v^2)v-Hv & -(\gamma-1)uv & H-(\gamma-1)v^2 & \gamma v & -(\gamma-1)qv \\ -vY & 0 & Y & 0 & v \end{pmatrix}.$$

It can be diagonalized as

$$\tilde{\mathsf{L}}_B\mathsf{B}\tilde{\mathsf{R}}_B = \mathrm{diag}(v, v, v, v+c, v-c)$$

with

(4.7)

$$\tilde{\mathsf{L}}_B = \begin{pmatrix} 1-\frac{\gamma-1}{2}\frac{u^2+v^2}{c^2} & (\gamma-1)\frac{u}{c^2} & (\gamma-1)\frac{v}{c^2} & -\frac{\gamma-1}{c^2} & q\frac{\gamma-1}{c^2} \\ -u & 1 & 0 & 0 & 0 \\ -\frac{\gamma-1}{2}\frac{u^2+v^2}{c^2}Y & (\gamma-1)\frac{u}{c^2}Y & (\gamma-1)\frac{v}{c^2}Y & -\frac{\gamma-1}{c^2}Y & 1+q\frac{\gamma-1}{c^2}Y \\ \frac{\gamma-1}{4}\frac{u^2+v^2}{c^2}-\frac{1}{2}\frac{v}{c} & -\frac{\gamma-1}{2}\frac{u}{c^2} & -\frac{\gamma-1}{2}\frac{v}{c^2}+\frac{1}{2c} & \frac{\gamma-1}{2c^2} & -q\frac{\gamma-1}{2c^2} \\ \frac{\gamma-1}{4}\frac{u^2+v^2}{c^2}+\frac{1}{2}\frac{v}{c} & -\frac{\gamma-1}{2}\frac{u}{c^2} & -\frac{\gamma-1}{2}\frac{v}{c^2}-\frac{1}{2c} & \frac{\gamma-1}{2c^2} & -q\frac{\gamma-1}{2c^2} \end{pmatrix},$$

$$\tilde{\mathsf{R}}_B = \tilde{\mathsf{L}}_B^{-1} = \begin{pmatrix} 1 & 0 & 0 & 1 & 1 \\ u & 1 & 0 & u & u \\ v & 0 & 0 & v+c & v-c \\ \frac{1}{2}(u^2+v^2) & u & q & H+vc & H-vc \\ 0 & 0 & 1 & Y & Y \end{pmatrix}.$$

It is direct to compute that

$$\mathsf{G}^2 := \tilde{\mathsf{L}}_A^{-T}\eta_{UU}\tilde{\mathsf{L}}_A^{-1} = \tilde{\mathsf{L}}_B^{-T}\eta_{UU}\tilde{\mathsf{L}}_B^{-1} = \mathrm{diag}(\mathsf{C}, \frac{2\gamma}{\rho}, \frac{2\gamma}{\rho}),$$

$$\mathsf{C} = \begin{pmatrix} \frac{\gamma}{\gamma-1}\frac{1}{\rho} + 2\frac{Y^2}{\rho} & 0 & -2\frac{Y}{\rho} \\ 0 & \frac{1}{p} & 0 \\ -2\frac{Y}{\rho} & 0 & \frac{2}{\rho} \end{pmatrix}.$$

The 3×3 matrix C can be diagonalized as $\mathsf{C} = \mathsf{M}\,\mathrm{diag}(\zeta_1, \zeta_2, \frac{1}{p})\mathsf{M}^T$, where $\zeta_1, \zeta_2 = \frac{1}{\rho}(\frac{3\gamma-2}{2\gamma-2} + Y^2) \pm \frac{1}{\rho}\sqrt{(\frac{3\gamma-2}{2\gamma-2} + Y^2)^2 - \frac{2\gamma}{\gamma-1}}$ and M is a unitary matrix given by

$$\mathsf{M} = \begin{pmatrix} \frac{\zeta_1\rho-2}{\sqrt{(\zeta_1\rho-2)^2+4Y^2}} & \frac{\zeta_2\rho-2}{\sqrt{(\zeta_2\rho-2)^2+4Y^2}} & 0 \\ 0 & 0 & 1 \\ \frac{2Y}{\sqrt{(\zeta_1\rho-2)^2+4Y^2}} & \frac{2Y}{\sqrt{(\zeta_2\rho-2)^2+4Y^2}} & 0 \end{pmatrix}.$$

Then we have

$$\mathsf{C}^{-\frac{1}{2}} = \mathsf{M}\,\mathrm{diag}(\frac{1}{\sqrt{\zeta_1}}, \frac{1}{\sqrt{\zeta_2}}, \sqrt{p})\mathsf{M}^T := \begin{pmatrix} g_1 & 0 & g_2 \\ 0 & \sqrt{p} & 0 \\ g_2 & 0 & g_3 \end{pmatrix}$$

and

$$\mathsf{R}_A = \tilde{\mathsf{R}}_A\mathsf{G}^{-1} = \begin{pmatrix} g_1 & 0 & g_2 & \sqrt{\frac{\rho}{2\gamma}} & \sqrt{\frac{\rho}{2\gamma}} \\ ug_1 & 0 & ug_2 & (u+c)\sqrt{\frac{\rho}{2\gamma}} & (u-c)\sqrt{\frac{\rho}{2\gamma}} \\ vg_1 & \sqrt{p} & vg_2 & v\sqrt{\frac{\rho}{2\gamma}} & v\sqrt{\frac{\rho}{2\gamma}} \\ \frac{1}{2}(u^2+v^2)g_1 + qg_2 & v\sqrt{p} & \frac{1}{2}(u^2+v^2)g_2 + qg_3 & (H+uc)\sqrt{\frac{\rho}{2\gamma}} & (H-uc)\sqrt{\frac{\rho}{2\gamma}} \\ g_2 & 0 & g_3 & Y\sqrt{\frac{\rho}{2\gamma}} & Y\sqrt{\frac{\rho}{2\gamma}} \end{pmatrix},$$

$$\mathsf{R}_B = \tilde{\mathsf{R}}_B\mathsf{G}^{-1} = \begin{pmatrix} g_1 & 0 & g_2 & \sqrt{\frac{\rho}{2\gamma}} & \sqrt{\frac{\rho}{2\gamma}} \\ ug_1 & \sqrt{p} & ug_2 & u\sqrt{\frac{\rho}{2\gamma}} & u\sqrt{\frac{\rho}{2\gamma}} \\ vg_1 & 0 & vg_2 & (v+c)\sqrt{\frac{\rho}{2\gamma}} & (v-c)\sqrt{\frac{\rho}{2\gamma}} \\ \frac{1}{2}(u^2+v^2)g_1 + qg_2 & u\sqrt{p} & \frac{1}{2}(u^2+v^2)g_2 + qg_3 & (H+vc)\sqrt{\frac{\rho}{2\gamma}} & (H-vc)\sqrt{\frac{\rho}{2\gamma}} \\ g_2 & 0 & g_3 & Y\sqrt{\frac{\rho}{2\gamma}} & Y\sqrt{\frac{\rho}{2\gamma}} \end{pmatrix},$$

which satisfy $\mathsf{R}_A\mathsf{R}_A^T = \mathsf{R}_B\mathsf{R}_B^T = \eta_{UU}^{-1}$. With R_A and R_B, the dissipation matrices can be computed as for the 1D case (see subsection 3.2).

Having the two-point entropy preserving fluxes and dissipation matrices, we can directly construct high-order entropy preserving/stable schemes in two dimensions. The construction is the same as for the 1D case and we refer to e.g. [35] for the details.

5. Numerical results

This section is devoted to the validation of our entropy preserving/stable schemes based on both the Tadmor flux and the KEP flux for 1D and 2D reactive Euler equations. For simplicity, we only take $k = 3$ and validate the sixth-order entropy preserving scheme and the fifth-order entropy stable scheme with (fifth-order) WENO reconstruction, which are referred to as EP6 and ES5, respectively. The third-order implicit-explicit Runge-Kutta method in [1] is employed for the time discretization. Four examples are used to demonstrate the designed accuracy of all the schemes as well as the ability of entropy stable schemes for problems with

discontinuities. In all the examples, the parameters of the reactive Euler equations are chosen following [13, 33]:

$$\gamma = 1.2, \quad q = 50, \quad \tilde{T} = 50, \quad \tilde{K} = 2566.4.$$

Except for Example 2, periodic boundary conditions are employed to avoid the effect of boundaries.

Example 1 (1D smooth problem)**.** We first test the accuracy of our schemes through a 1D smooth problem with exact solution

$$\rho = 1 + 0.3\sin(2\pi(x-t)), \quad u = 1, \quad p = 1, \quad Y = 0 \tag{5.1}$$

in the domain $[0, 1]$. We take the mesh size as $\Delta x = 1/20, 1/40, 1/80, 1/160$ and set $\Delta t = \Delta x^2$ and $\Delta t = \Delta x^{5/3}$ for the EP6 and ES5, respectively. The L^1 and L^∞ errors at $t = 0.1$ are listed in Table 1. We observe that for both the Tadmor flux and the KEP flux the designed sixth- and fifth-order convergence is obtained for the EP6 and ES5 scheme, respectively. Additionally, the errors of the two fluxes are very close and have the same values at the first decimal place.

TABLE 1. Error table for 1D smooth problem with exact solution (5.1)

Tadmor flux	EP6			
Δx	L^1 error	order	L^∞ error	order
1/20	2.7360e-06		9.3507e-06	
1/40	4.8079e-08	5.8305	1.9061e-07	5.6164
1/80	7.7813e-10	5.9493	3.1416e-09	5.9230
1/160	1.2265e-11	5.9874	4.9729e-11	5.9813
Tadmor flux	ES5			
Δx	L^1 error	order	L^∞ error	order
1/20	2.0015e-04		4.3710e-04	
1/40	2.5855e-05	2.9525	5.3814e-05	3.0219
1/80	1.5148e-06	4.0933	3.7037e-06	3.8610
1/160	1.6687e-08	6.5042	4.7931e-08	6.2719
KEP flux	EP6			
Δx	L^1 error	order	L^∞ error	order
1/20	2.7362e-06		9.3508e-06	
1/40	4.8077e-08	5.8306	1.9061e-07	5.6164
1/80	7.7812e-10	5.9492	3.1416e-09	5.9230
1/160	1.2266e-11	5.9873	4.9733e-11	5.9811
KEP flux	EP5			
Δx	L^1 error	order	L^∞ error	
1/20	2.0148e-04		4.1394e-04	
1/40	2.5574e-05	2.9778	5.3044e-05	2.9642
1/80	1.5086e-06	4.0834	3.7063e-06	3.8391
1/160	1.6687e-08	6.4983	4.7875e-08	6.2746

Example 2 (1D problem with discontinuities)**.** In this test, we consider the Riemann type initial conditions

$$(\rho, u, p, Y) = \begin{cases} (1, 0, 1, 0) & \text{if } x < 0, \\ (0.125, 0, 0.1, 0) & \text{if } x > 0, \end{cases} \tag{5.2}$$

where the initial data of ρ, u, p are the same as those of Sod's problem for the Euler equations [29]. The computational domain is $[-5, 5]$ and we take the mesh size as $\Delta x = 1/16$. The numerical solutions at $t = 2$ with CFL=0.5 for the ES5 scheme are plotted in Fig. 1. It can be seen that the results of the Tadmor flux and the KEP flux are almost the same and the discontinuities are well captured without oscillations. As expected, the total numerical entropy $\sum_i \hat{\eta}(U_i(t))\Delta x$ decreases with respect to time; see Fig. 2. We also observe from Fig. 1 that the reactant mass fraction Y oscillates slightly and becomes negative around the contact discontinuity. The magnitude of the oscillation is reduced under a smaller mesh size $\Delta x = 1/160$ in our numerical experiments. These indicate that the present schemes do not guarantee the positivity of Y. Enforcing both the positivity of solution and the ES property will be our next target.

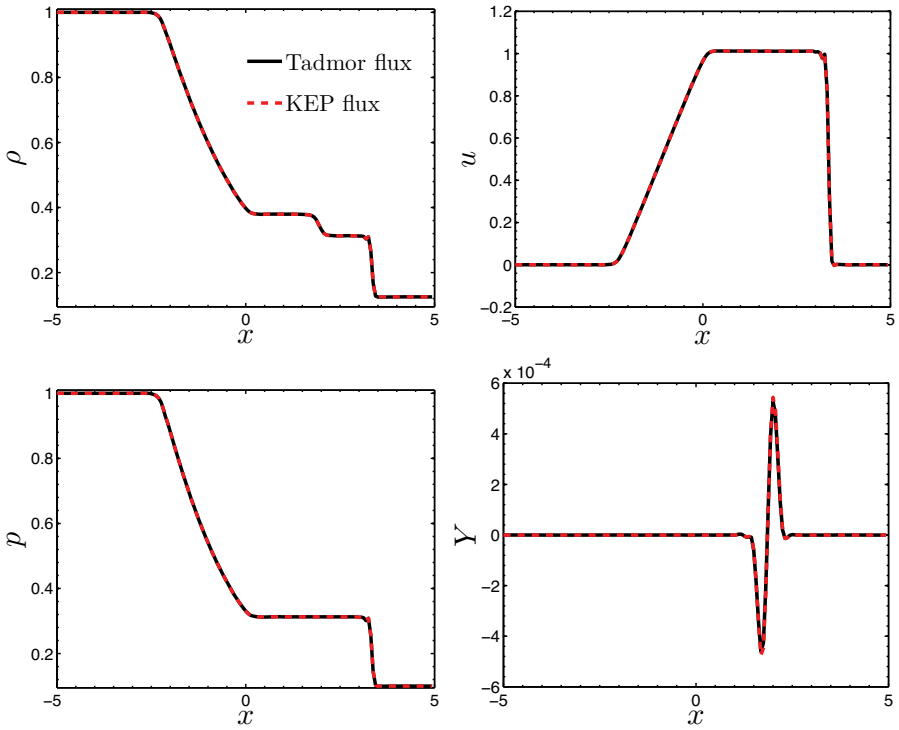

FIGURE 1. Example 2: Computational results at $t = 2$ with $\Delta x = 1/16$

Example 3 (2D smooth problem)**.** In the following, we validate our schemes for 2D problems. As for the 1D case, we first test the accuracy with the exact solution

$$\rho = 1 + 0.3\sin(2\pi(x + y - t)), \quad u = 1, \quad v = 0, \quad p = 1, \quad Y = 0 \tag{5.3}$$

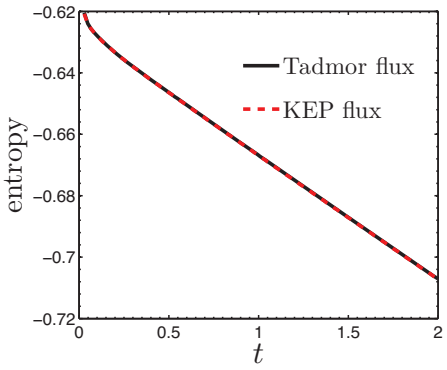

FIGURE 2. Example 2: Evolution of the total numerical entropy

in a square domain $[0,1]\times[0,1]$. The mesh sizes are $\Delta x = 1/20, 1/40, 1/80, 1/160$ and the time steps are $\Delta t = \Delta x^2, \Delta x^{5/3}$ for the EP6 and ES5, respectively. Table 2 lists the errors at $t = 0.01$, from which designed convergence orders can be observed for both the Tadmor flux and the KEP flux. Similar to the 1D case, the errors of the two fluxes are also very close. These demonstrate the accuracy of our schemes for 2D problems.

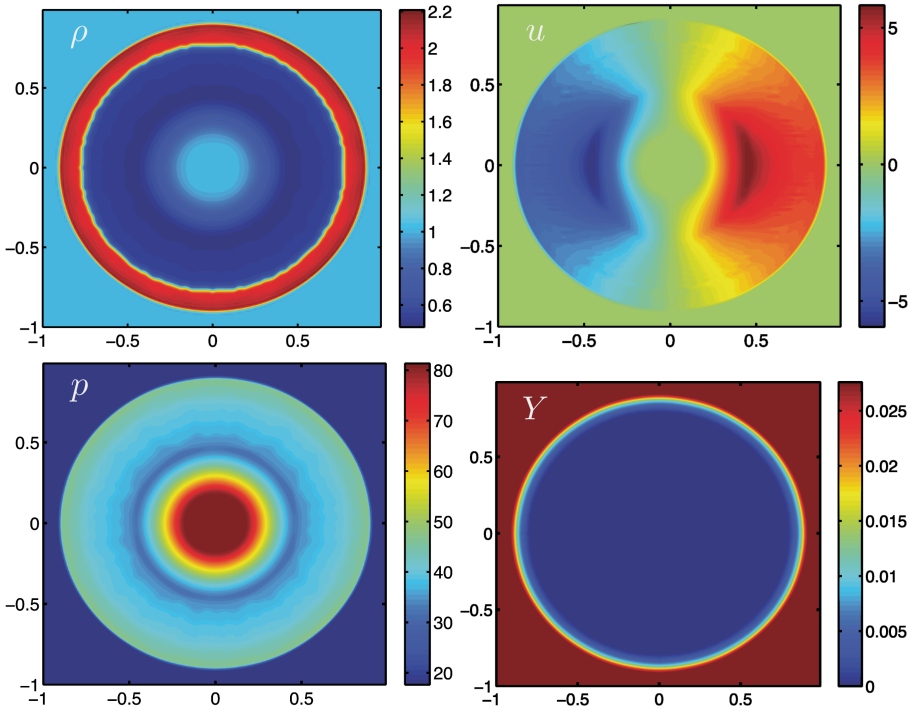

FIGURE 3. Example 4: Contours of different variables at $t = 0.04$

TABLE 2. Error table for 2D smooth problem with exact solution (5.3)

Tadmor flux	EP6			
Δx	L^1 error	order	L^∞ error	order
1/20	2.7913e-07		1.0150e-06	
1/40	4.8688e-09	5.8412	1.9297e-08	5.7170
1/80	7.7978e-11	5.9643	3.1515e-10	5.9361
1/160	1.2275e-12	5.9893	4.9808e-12	5.9835
Tadmor flux	EP5			
Δx	L^1 error	order	L^∞ error	order
1/20	8.4400e-05		2.5753e-04	
1/40	9.2748e-06	3.1858	3.8804e-05	2.7305
1/80	4.1865e-07	4.4695	2.1626e-06	4.1654
1/160	8.9274e-09	5.5514	4.4572e-08	5.6005
KEP flux	EP6			
Δx	L^1 error	order	L^∞ error	order
1/20	2.7914e-07		1.0150e-06	
1/40	4.8686e-09	5.8414	1.9296e-08	5.7170
1/80	7.7978e-11	5.9643	3.1515e-10	5.9361
1/160	1.2275e-12	5.9892	4.9812e-12	5.9834
KEP flux	EP5			
Δx	L^1 error	order	L^∞ error	order
1/20	8.5440e-05		3.3197e-04	
1/40	8.8719e-06	3.2676	3.0030e-05	3.4666
1/80	4.2291e-07	4.3908	2.2207e-06	3.7573
1/160	8.8464e-09	5.5791	4.6625e-08	5.5737

Example 4 (2D problem with discontinuities)**.** In this example, we test our schemes for a 2D problem containing discontinuities. The computational domain is $[-1,1]\times[-1,1]$ and the initial data is given by

$$(\rho,u,v,p,Y)=\begin{cases}(1,0,0,80,0.2), & x^2+y^2\le 0.36,\\ (1,0,0,10,0.8), & \text{otherwise},\end{cases} \tag{5.4}$$

which is taken from [39]. In the computation we employ the ES5 scheme with a mesh size $\Delta x = 1/100$ and $CFL = 0.2$. Again, the results of the Tadmor flux and the KEP flux are very similar. The contour plots of ρ, u, p, Y at $t = 0.04$ obtained with the Tadmor flux are given in Fig. 3 and the solutions along the horizontal line $y = 0$ are plotted in Fig. 4. We see that the von Neumann spike is clearly resolved. Additionally, as shown in Fig. 5 the total numerical entropy $\sum_{i,j}\hat{\eta}(U_{i,j}(t))\Delta x$ decreases with respect to time, supporting that our schemes are entropy stable.

6. Conclusions and remarks

In this paper, we present entropy analysis and high-order ES finite difference schemes for the reactive Euler equations in both one- and two-dimensions on a Cartesian mesh. First, we show that the thermodynamic entropy is no longer strictly convex for the reactive Euler equations. To address this issue, we propose

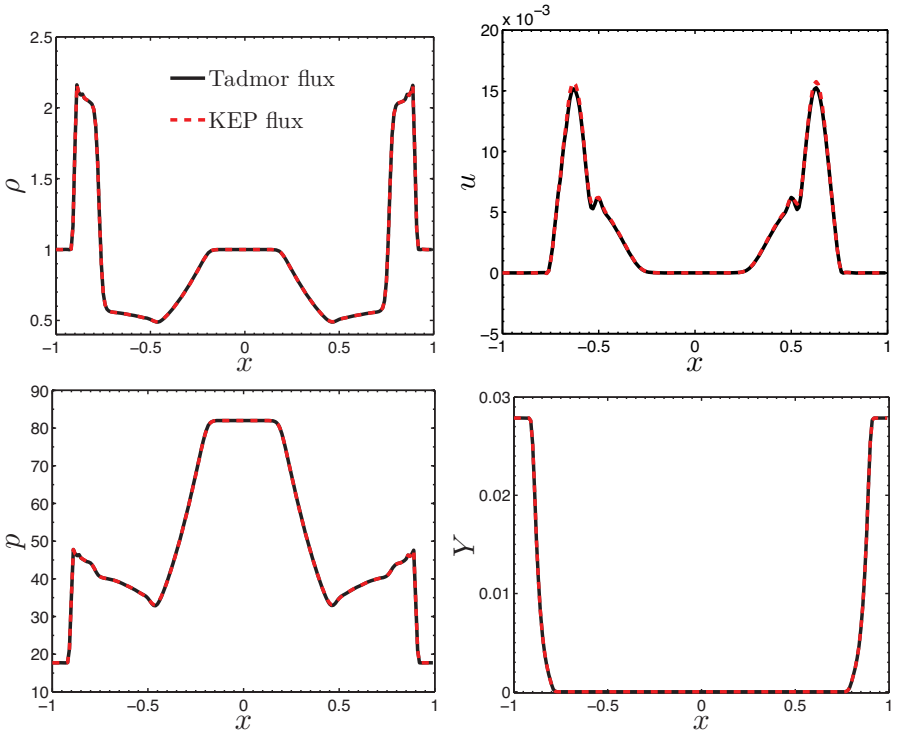

FIGURE 4. Example 4: Solutions along the horizontal line $y = 0$

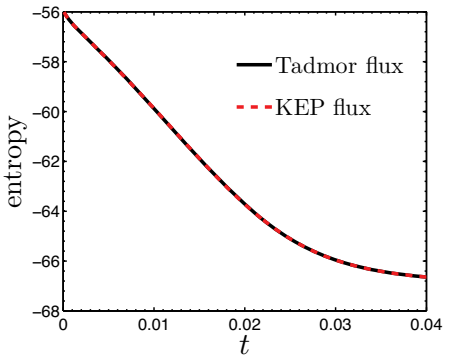

FIGURE 5. Example 4: Evolution of the total numerical entropy

a strictly convex entropy function by adding an extra term to the thermodynamic entropy. As a result, a new entropy-entropy flux pair is obtained. Thanks to the strict convexity of the proposed entropy, the Roe-type dissipation operator in terms of the entropy variables can be formulated [28]. Note that such dissipation operators are not available based on the thermodynamic entropy, as it is not strictly convex.

Furthermore, we construct two sets of second-order EP fluxes by extending those in [5, 28] for the Euler equations within the framework of [31]. In particular, the

EP fluxes extended from [5] are also KEP. With the EP fluxes and the Roe-type dissipation operators, high-order EP/EC fluxes are derived following [17, 25], where the sign-preserving ENO [16] and WENO [3] reconstructions are employed for the high-order dissipation operators. Numerical experiments in 1D and 2D validate the designed accuracy and good performance for smooth and discontinuous problems. The entropy decrease of ES schemes is verified as well.

We would like to point out that for the reactive Euler equations as hyperbolic balance laws, the strict convexity of entropy function is crucial for the global existence of solution [36]. The present strictly convex entropy may be helpful for the theoretical analysis of the reactive Euler equations. On the other hand, we observe that the proposed schemes do not guarantee the positivity of the reactant mass fraction. This may be overcome with the positivity limiters in [37, 38]. These will be the topic of our work in the future.

References

[1] U. M. Ascher, S. J. Ruuth, and R. J. Spiteri, *Implicit-explicit Runge-Kutta methods for time-dependent partial differential equations*, Appl. Numer. Math. **25** (1997), no. 2-3, 151–167, DOI 10.1016/S0168-9274(97)00056-1. Special issue on time integration (Amsterdam, 1996). MR1485812

[2] T. J. Barth, *Numerical methods for gasdynamic systems on unstructured meshes*, An Introduction to Recent Developments in Theory and Numerics for Conservation Laws (Freiburg/Littenweiler, 1997), Lect. Notes Comput. Sci. Eng., vol. 5, Springer, Berlin, 1999, pp. 195–285, DOI 10.1007/978-3-642-58535-7_5. MR1731618

[3] B. Biswas and R. K. Dubey, *Low dissipative entropy stable schemes using third order WENO and TVD reconstructions*, Adv. Comput. Math. **44** (2018), no. 4, 1153–1181, DOI 10.1007/s10444-017-9576-2. MR3842951

[4] A. Bourlioux, A. J. Majda, and V. Roytburd, *Theoretical and numerical structure for unstable one-dimensional detonations*, SIAM J. Appl. Math. **51** (1991), no. 2, 303–343, DOI 10.1137/0151016. MR1095022

[5] P. Chandrashekar, *Kinetic energy preserving and entropy stable finite volume schemes for compressible Euler and Navier-Stokes equations*, Commun. Comput. Phys. **14** (2013), no. 5, 1252–1286, DOI 10.4208/cicp.170712.010313a. MR3079107

[6] P. Chandrashekar and C. Klingenberg, *Entropy stable finite volume scheme for ideal compressible MHD on 2-D Cartesian meshes*, SIAM J. Numer. Anal. **54** (2016), no. 2, 1313–1340, DOI 10.1137/15M1013626. MR3490501

[7] G.-Q. Chen and D. H. Wagner, *Global entropy solutions to exothermically reacting, compressible Euler equations*, J. Differential Equations **191** (2003), no. 2, 277–322, DOI 10.1016/S0022-0396(03)00027-5. MR1978380

[8] T. Chen and C.-W. Shu, *Entropy stable high order discontinuous Galerkin methods with suitable quadrature rules for hyperbolic conservation laws*, J. Comput. Phys. **345** (2017), 427–461, DOI 10.1016/j.jcp.2017.05.025. MR3667622

[9] J. F. Clarke, S. Karni, J. J. Quirk, P. L. Roe, L. G. Simmonds, and E. F. Toro, *Numerical computation of two-dimensional unsteady detonation waves in high energy solids*, J. Comput. Phys. **106** (1993), no. 2, 215–233.

[10] P. Colella, A. Majda, and V. Roytburd, *Theoretical and numerical structure for reacting shock waves*, SIAM J. Sci. Statist. Comput. **7** (1986), no. 4, 1059–1080, DOI 10.1137/0907073. MR857783

[11] J. Duan and H. Tang, *High-order accurate entropy stable finite difference schemes for one- and two-dimensional special relativistic hydrodynamics*, Adv. Appl. Math. Mech. **12** (2020), no. 1, 1–29, DOI 10.4208/aamm.oa-2019-0124. MR4048875

[12] W. Fickett, *Detonations in miniature*, University of California Press, Berkeley, 1985.

[13] W. Fickett and W. W. Wood, *Flow calculations for pulsating one dimensional detonations*, Phys. Fluids **9** (1966), no. 5, 903–916.

[14] T. C. Fisher and M. H. Carpenter, *High-order entropy stable finite difference schemes for nonlinear conservation laws: finite domains*, J. Comput. Phys. **252** (2013), 518–557, DOI 10.1016/j.jcp.2013.06.014. MR3101520

[15] U. S. Fjordholm, S. Mishra, and E. Tadmor, *Energy preserving and energy stable schemes for the shallow water equations*, Foundations of Computational Mathematics, Hong Kong 2008, London Math. Soc. Lecture Note Ser., vol. 363, Cambridge Univ. Press, Cambridge, 2009, pp. 93–139. MR2562498

[16] U. S. Fjordholm, S. Mishra, and E. Tadmor, *Arbitrarily high-order accurate entropy stable essentially nonoscillatory schemes for systems of conservation laws*, SIAM J. Numer. Anal. **50** (2012), no. 2, 544–573, DOI 10.1137/110836961. MR2914275

[17] U. S. Fjordholm, S. Mishra, and E. Tadmor, *ENO reconstruction and ENO interpolation are stable*, Found. Comput. Math. **13** (2013), no. 2, 139–159, DOI 10.1007/s10208-012-9117-9. MR3032678

[18] L. Friedrich, G. Schnücke, A. R. Winters, D. C. Del Rey Fernández, G. J. Gassner, and M. H. Carpenter, *Entropy stable space-time discontinuous Galerkin schemes with summation-by-parts property for hyperbolic conservation laws*, J. Sci. Comput. **80** (2019), no. 1, 175–222, DOI 10.1007/s10915-019-00933-2. MR3954440

[19] G. J. Gassner, *A skew-symmetric discontinuous Galerkin spectral element discretization and its relation to SBP-SAT finite difference methods*, SIAM J. Sci. Comput. **35** (2013), no. 3, A1233–A1253, DOI 10.1137/120890144. MR3048217

[20] G. Hu, *A numerical study of 2D detonation waves with adaptive finite volume methods on unstructured grids*, J. Comput. Phys. **331** (2017), 297–311, DOI 10.1016/j.jcp.2016.11.041. MR3588693

[21] J. Huang, W. Zhao, and C.-W. Shu, *A third-order unconditionally positivity-preserving scheme for production-destruction equations with applications to non-equilibrium flows*, J. Sci. Comput. **79** (2019), no. 2, 1015–1056, DOI 10.1007/s10915-018-0881-9. MR3969000

[22] F. Ismail and P. L. Roe, *Affordable, entropy-consistent Euler flux functions. II. Entropy production at shocks*, J. Comput. Phys. **228** (2009), no. 15, 5410–5436, DOI 10.1016/j.jcp.2009.04.021. MR2541460

[23] A. Jameson, *Formulation of kinetic energy preserving conservative schemes for gas dynamics and direct numerical simulation of one-dimensional viscous compressible flow in a shock tube using entropy and kinetic energy preserving schemes*, J. Sci. Comput. **34** (2008), no. 2, 188–208, DOI 10.1007/s10915-007-9172-6. MR2373037

[24] D. D. Knight, *Elements of Numerical Methods for Compressible Flows*, Cambridge Aerospace Series, vol. 19, Cambridge University Press, Cambridge, 2006, DOI 10.1017/CBO9780511617447. MR2267852

[25] P. G. Lefloch, J. M. Mercier, and C. Rohde, *Fully discrete, entropy conservative schemes of arbitrary order*, SIAM J. Numer. Anal. **40** (2002), no. 5, 1968–1992, DOI 10.1137/S003614290240069X. MR1950629

[26] S. Osher, *Riemann solvers, the entropy condition, and difference approximations*, SIAM J. Numer. Anal. **21** (1984), no. 2, 217–235, DOI 10.1137/0721016. MR736327

[27] S. Osher and E. Tadmor, *On the convergence of difference approximations to scalar conservation laws*, Math. Comp. **50** (1988), no. 181, 19–51, DOI 10.2307/2007913. MR917817

[28] P. L. Roe, *Affordable, entropy consistent flux functions*, Eleventh International Conference on Hyperbolic Problems: Theory, Numerics and Applications, 2006.

[29] G. A. Sod, *A survey of several finite difference methods for systems of nonlinear hyperbolic conservation laws*, J. Comput. Phys. **27** (1978), no. 1, 1–31, DOI 10.1016/0021-9991(78)90023-2. MR495002

[30] P. K. Subbareddy and G. V. Candler, *A fully discrete, kinetic energy consistent finite-volume scheme for compressible flows*, J. Comput. Phys. **228** (2009), no. 5, 1347–1364, DOI 10.1016/j.jcp.2008.10.026. MR2494220

[31] E. Tadmor, *The numerical viscosity of entropy stable schemes for systems of conservation laws. I*, Math. Comp. **49** (1987), no. 179, 91–103, DOI 10.2307/2008251. MR890255

[32] E. Tadmor, *Entropy stability theory for difference approximations of nonlinear conservation laws and related time-dependent problems*, Acta Numer. **12** (2003), 451–512, DOI 10.1017/S0962492902000156. MR2249160

[33] C. Wang, X. Zhang, C.-W. Shu, and J. Ning, *Robust high order discontinuous Galerkin schemes for two-dimensional gaseous detonations*, J. Comput. Phys. **231** (2012), no. 2, 653–665, DOI 10.1016/j.jcp.2011.10.002. MR2872096

[34] A. R. Winters and G. J. Gassner, *Affordable, entropy conserving and entropy stable flux functions for the ideal MHD equations*, J. Comput. Phys. **304** (2016), 72–108, DOI 10.1016/j.jcp.2015.09.055. MR3422404

[35] K. Wu and C.-W. Shu, *Entropy symmetrization and high-order accurate entropy stable numerical schemes for relativistic MHD equations*, SIAM J. Sci. Comput. **42** (2020), no. 4, A2230–A2261, DOI 10.1137/19M1275590. MR4125873

[36] W.-A. Yong, *Entropy and global existence for hyperbolic balance laws*, Arch. Ration. Mech. Anal. **172** (2004), no. 2, 247–266, DOI 10.1007/s00205-003-0304-3. MR2058165

[37] X. Zhang and C.-W. Shu, *Positivity-preserving high order discontinuous Galerkin schemes for compressible Euler equations with source terms*, J. Comput. Phys. **230** (2011), no. 4, 1238–1248, DOI 10.1016/j.jcp.2010.10.036. MR2753359

[38] X. Zhang and C.-W. Shu, *Positivity-preserving high order finite difference WENO schemes for compressible Euler equations*, J. Comput. Phys. **231** (2012), no. 5, 2245–2258, DOI 10.1016/j.jcp.2011.11.020. MR2876636

[39] W. Zhao and J. Huang, *Boundary treatment of implicit-explicit Runge-Kutta method for hyperbolic systems with source terms*, J. Comput. Phys. **423** (2020), 109828, 22, DOI 10.1016/j.jcp.2020.109828. MR4157647

Department of Applied Mathematics, University of Science and Technology Beijing, Beijing 100083, People's Republic of China

Email address: wfzhao@ustb.edu.cn